

DESIGN AND OPTIMIZATION OF SOLAR POWER
PLANT CONSISTED OF TRACKING CONCENTRATOR
PHOTOVOLTAIC SYSTEM BASED ON
COMPUTATIONAL ANALYSIS

OOON LI VOON

MASTER OF ENGINEERING SCIENCE

LEE KONG CHIAN FACULTY OF ENGINEERING SCIENCE

UNIVERSITY TUNKU ABDUL RAHMAN

MARCH 2021

**DESIGN AND OPTIMIZATION OF SOLAR POWER PLANT
CONSISTED OF TRACKING CONCENTRATOR PHOTOVOLTAIC
SYSTEM BASED ON COMPUTATIONAL ANALYSIS**

By

OON LI VOON

A dissertation submitted to the Department of Electrical and Electronics Engineering, Lee Kong Chian Faculty of Engineering Science, University Tunku Abdul Rahman, in partial fulfillment of the requirements for the degree of Master of Engineering Science.

MARCH 2021

ABSTRACT

DESIGN AND OPTIMIZATION OF SOLAR POWER PLANT CONSISTED OF TRACKING CONCENTRATOR PHOTOVOLTAIC SYSTEM BASED ON COMPUTATIONAL ANALYSIS

Oon Li Voon

The deterioration of overall electrical generation of solar power plant (SPP) as a result of optical losses via shadowing between adjacent CPV systems. The optical losses occur due to an inappropriate distribution of space for concentrator photovoltaic system (CPV) systems in the solar farm. An increase in the separation distance between adjacent CPV systems can reduce the deterioration of the overall electrical generation. Although this method can solve the existing problem, this causes an increase in land-related costs as a result of the ineffectiveness in land utilization. Thus, optimization of the layout design in the SPP is crucial towards the achievement of the best trade-off between land utilization and energy generation. The levelized cost of electricity (LCOE) of the SPP must be competitive in solar energy field to garner the interest from possible investors for its future development. In this research work, a newly developed computational algorithm has been presented to carry out the CPV field layout optimization process. This algorithm utilizes the local meteorological data, including the consideration of shadowing effect, land aspect ratio (LAR) and the cost of land. In this dissertation, a case study has been conducted in Kota Kinabalu, Malaysia based on different condition

such as D_{ew}/L ratio, D_{ns}/L ratio, LAR and land cost to assess the performance of CPV system in the SPP for both square array and staggered array configuration. According to the results obtained through the case study, the optimized field layout for CPV systems for LAR of 1 is a staggered array layout configuration with the D_{ew}/L ratio of 2.50 at spacing angle of 45 degree, which holds the lowest value of LCOE.

ACKNOWLEDGEMENT

This thesis is prepared as a partial requirement for the degree of Master of Engineering Science in University Tunku Abdul Rahman. The successful production of this report involves many valuable contributions from a number of parties and as a token of appreciation I would like to dedicate this page to them.

I would like to express my greatest appreciation towards my current supervisor, Dr. Tan Ming Hui as well as my former co-supervisor, Dr. Wong Chee Woon. Their willingness to spare their time and patience are very much appreciated. I would also like to thank my current co-supervisor Prof. Chong Kok Keong for his encouragement, useful critiques and suggestions to improve this research work. This research work would not have been completed without the professional assistance from them. I would like to show my special thanks to my colleagues particularly Soon Kok Yew who helped me to revise and proofread my thesis. I am particularly grateful to my family for their moral and financial support. Finally, I would also like to thank the faculty and staffs of UTAR Institute of Postgraduate Studies and Research (IPSR) and Lee Kong Chian Faculty of Engineering & Science (LKC FES) for their assistances and expertise throughout my postgraduate research. I would like to express sincere gratitude to UTAR Research Fund 2017 Cycle 2 with project number IPSR/RMC/UTARRF/2017-C2/T04 (vote account 6200/TD5) for their financial support. In additions, I would also like to express gratitude to the Ministry of Energy, Green Technology and Water (AAIBE Trust Fund) with vote account 4356/001.

APPROVAL SHEET

This thesis/dissertation entitled “DESIGN AND OPTIMIZATION OF SOLAR POWER PLANT FIELD LAYOUT OF CONCENTRATOR PHOTOVOLTAIC SYSTEM BASED ON COMPUTATIONAL ANALYSIS” was prepared by OON LI VOON and submitted as partial fulfilment of the requirements for the degree of Master of Engineering Science at Universiti Tunku Abdul Rahman.

Approved by:

Nic

(Dr. TAN MING HUI)

Date: 1st March 2021.....

Main Supervisor

Department of Industrial Engineering

Faculty of Engineering and Green Technology

Universiti Tunku Abdul Rahman

K.K.Chong

(Prof. CHONG KOK KEONG)

Date: 2 March 2021.....

Professor / Co-supervisor

Department of Electrical and Electronic Engineering

Faculty of Engineering and Science

Universiti Tunku Abdul Rahman

**FACULTY OF ENGINEERING AND SCIENCE
UNIVERSITI TUNKU ABDUL RAHMAN**

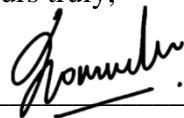
Date: 1 MARCH 2021

SUBMISSION OF THESIS

It is hereby certified that **Oon Li Voon** (ID No: 18UEM01071) has completed this thesis entitled “DESIGN AND OPTIMIZATION OF SOLAR POWER PLANT FIELD LAYOUT OF CONCENTRATOR PHOTOVOLTAIC SYSTEM BASED ON COMPUTATIONAL ANALYSIS” under the supervision of Dr. Tan Ming Hui (Supervisor) from the Department of Industrial Engineering, Faculty of Engineering and Green Technology, and Prof. Dr. Chong Kok Keong (Co-Supervisor) from the Department of Electrical and Electronics Engineering, Faculty of Engineering and Science.

I understand that the University will upload a softcopy of my thesis in pdf format into UTAR Institutional Repository, which may be made accessible to UTAR community and the public.

Yours truly,



(OON LI VOON)

DECLARATION

I, OON LI VOON hereby declare that this thesis is based on my original work except for quotations and citations which have been duly acknowledged. I also declare that it has not been previously or concurrently submitted for any other degree at UTAR or other institutions.

Name: OON LI VOON

Date: 1 MARCH 2021

TABLE OF CONTENTS

	Page
ABSTRACT	ii
ACKNOWLEDGEMENT	iii
APPROVAL SHEET	v
SUBMISSION OF THESIS	vi
DECLARATION	vii
TABLE OF CONTENTS	viii
LIST OF TABLES	x
LIST OF FIGURES	xi
LIST OF ABBREVIATIONS	xiv
CHAPTER	
1.0 INTRODUCTION	1
1.1 Problem statement and research objectives	4
1.2 Scope of research	5
1.3 Outline of thesis	6
2.0 LITERATURE REVIEW	7
2.1 Importance of sun-tracking (ST) system	7
2.1.1 Types of sun-tracking (ST) system	9
2.1.2 1 axis sun-tracking (ST) system	10
2.1.3 2 axis sun-tracking (ST) system	12
2.1.4 Justification on both sun-tracking (ST) system	14
2.1.5 Basic computations of sun position	15
2.2 Overall review of the electrical performance of PV/CPV system	19
2.3 Methods/Algorithm used by researchers on layout optimization	21
2.3.1 Geometry of mutual shadowing	21
2.3.2 Ray-tracing (point-to-point) method	22
2.3.3 Ray/Plane algorithm (Four-point method)	24

2.4	Research approach in the optimization of large solar power plant	24
2.5	Levelized cost of electricity (LCOE)	25
3.0	METHODOLOGY	27
3.1	Sun-tracking (ST) angles	30
3.2	Coordinate transformation	30
3.3	The Sun-incident ray and ray/plane algorithm	35
3.4	Levelized cost of electricity (LCOE)	36
3.5	Layout configuration	37
3.6	Annual energy generation	40
4.0	RESULT AND DISCUSSION	41
4.1	Shadowing	41
4.2	Annual energy generation	45
4.3	Levelized cost of electricity (LCOE)	48
4.4	Edge effect	52
4.5	Land-related cost	55
4.6	Land aspect ratio (LAR)	56
5.0	CONCLUSION AND FUTURE WORK	59
5.1	Conclusion	59
5.2	Future work	60
	REFERENCES	61
	PUBLICATIONS	67

LIST OF TABLES

Table		Page
2.1	Basic characteristics of each type of 1 axis sun-tracking system.	10
2.2	Basic characteristics of each type of 2 axis sun-tracking system.	12
2.3	Comparison between both sun-tracking systems (solarflexrack, 2013).	15
3.1	Specification of the CPV system solar power plant.	38
4.1	The most possible number of CPV systems to be fitted in the designated land area of 62,500 m ² for square array layout.	43
4.2	The most possible number of CPV systems to be fitted in the designated land area of 62,500 m ² for staggered array layout.	43
4.3	The parameters required in the calculation of LCOE of the solar farm consisted of CPV systems.	49
4.4	The optimal layout configuration for the cases of with and without considering the edge effect in the solar farm modelling.	55

LIST OF FIGURES

Figure		Page
2.1	Types of available sun-tracking (ST) system.	10
2.2	Applications of 1 axis sun-tracking (ST) system for solar PV panel (Rockwell Automation, 2011).	11
2.3	Applications of 1 axis sun-tracking (ST) system for solar thermal parabolic trough (Rockwell Automation, 2011).	12
2.4	Applications of 2 axis sun-tracking (ST) system for solar PV panel (Rockwell Automation, 2011).	13
2.5	Applications of 2 axis sun-tracking (ST) system for solar thermal dish (Rockwell Automation, 2011).	14
2.6	The variations of declination angle throughout the year (Lovegrove <i>et al.</i> , 2013).	16
2.7	The variations of hour angle throughout the day (Lovegrove <i>et al.</i> , 2013).	18
2.8	Position of elevation angle, α and azimuth angle, β (PVPerformance Modeling collaborative, no date).	19
2.9 (a)	Dimensions of a 2 axis tracker and length of its shadow (Perpiñán, 2012).	22
2.9 (b)	Mutual shadowing effect between six 2 ST system. (Perpiñán, 2012)	22
2.10	Figure 2.10: Ray-tracing method for shadow loss, where H is the horizon (represented by a sphere), G is the ground, D is the isotropic rectangular source and T are the sun tracking	23

	system that will shade the source (Oliveira Fartaria and Collares Pereira, 2013).	
2.11	Shadowing effect on “Test Heliostat”. (Chong and Tan, 2012)	24
3.1	Methodology of computational algorithm for optimizing the square array layout configuration.	28
3.2	Methodology of computational algorithm for optimizing the staggered array layout configuration of CPV field in MATLAB simulation platform.	29
3.3	The point-focus Fresnel lens CPV system that is used in the modelling of CPV farm layout (Muñoz <i>et al.</i> , 2010).	32
3.4	The initial coordinate for a structural frame of individual CPV system is defined in a local coordinate system, where the origin is defined at the center of structural frame of the CPV system and P_i is the corner edge point of structural frame of the CPV system.	33
3.5	Figure 3.5: The origin, $\mathbf{O}(0,0,0)$, of global coordinate system is defined as the centre of the CPV field. The final coordinate of structural frame of the CPV system is defined as $C (H_{cx}, H_{cy}, H_{cz})$ after performing the coordinate transformation.	33
3.6	Area of shadow caused by adjacent CPV system is computed using the ray/plane algorithm after performing the coordinate transformation for both CPV systems.	36

3.7	Schematic diagram for square array layout of the solar CPV farm.	39
3.8	Schematic diagram for staggered array layout of the solar CPV farm.	39
4.1	The annual average percentage of shadowing area (%) for square array layout.	44
4.2	The annual average percentage of shadowing area (%) for staggered array layout. The results were taken from its minimum D_{ew}/L ratio for each angle to avoid collision between adjacent CPV systems. The iteration of simulation algorithm will not be continued when the LCOE increases with the increment in the D_{ew}/L ratio to save the computational time.	45
4.3	The annual energy generation per CPV system (kWh) and the annual energy generation (GWh) for square array layout.	46
4.4	The annual energy generation per CPV system (kWh) and the annual energy generation (GWh) for staggered array layout. The results were taken from its minimum D_{ew}/L ratio for each angle to avoid collision between adjacent CPV systems. The iteration of simulation algorithm will not be continued when the LCOE increases with the increment in the D_{ew}/L ratio to save the computational time.	47
4.5	The ground coverage ratio (GCR) and LCOE (US\$/kWh) for square array layout at $LAR = 1$.	50

- 4.6 The ground coverage ratio (GCR) and LCOE (US\$/kWh) for staggered array layout at LAR = 1. The results were taken from its minimum D_{ew}/L ratio for each angle to avoid collision between adjacent CPV systems. The iteration of simulation algorithm will not be continued when the LCOE increases with the increment in the D_{ew}/L ratio to save the computational time. 51
- 4.7 The relationship between the annual energy generation, LCOE, square array layout configuration (D_{ew}/L , D_{ns}/L , GCR) and staggered array layout configuration (D_{ew}/L , Angle, GCR) at different LAR. 58

LIST OF ABBREVIATIONS

A	Total collector area of each CPV system (m^2)
A_s	Area of shadow (m^2)
A_T	Area of test CPV system (m^2)
d	Degradation rate of the CPV systems
BL	Bottom left
BR	Bottom right
CPV	Concentrator Photovoltaic
D_{ew}	Spacing distance between the CPV systems in East-West direction (m)

D_{ns}	Spacing distance between the CPV systems in North-South direction (m)
DNI	Direct normal irradiance, (W/m^2)
F_t	Interest expenditures of the CPV systems for t years (%)
GCR	Ground-cover ratio
GF	General formula
H_z	Height of the CPV system (m)
i	Number of days
I_t	Initial capital cost of the CPV systems (\$)
j	Number of time intervals per day
L	Dimension of a solar collector (m)
LAR	Land aspect ratio
LCOE	Levelized cost of electricity
l_{EW}	Length of land (m)
l_{NS}	Width of land (m)
M_t	Maintenance costs of the CPV systems for t years (\$)
O_t	Operational costs of the CPV systems for t years (\$)
S	Incident sunrays
S_t	Yearly rated energy output of the CPV systems for t years (kWh)
ST	Sun-tracking
T	Lifespan of the project (years)
TL	Top left
TR	Top right
t	Number of years
t_s	Solar time

Greek symbols:

α	elevation angle (°)
α_s	solar elevation angle (°)
β	azimuth angle (°)
β_s	solar azimuth angle (°)
η	power conversion efficiency of CPV system (%)
η_s	shadow efficiency (%)
ω	hour angle (°)
Φ	latitude (°)
δ	sun declination angle (°)
θ	spacing angle (°)

Subscripts:

<i>ew</i>	East - West
<i>ns</i>	North - South
<i>x</i>	<i>x</i> -direction
<i>y</i>	<i>y</i> -direction
<i>z</i>	<i>z</i> -direction

CHAPTER 1

INTRODUCTION

A noteworthy improvement in the power conversion efficiency of multijunction solar cell to 46% managed to garner the interest in concentrator photovoltaic (CPV) systems as an alternative to the conventional solar power generating system (Green *et al.*, 2019). The CPV system uses either lenses or reflectors to focus the sunlight onto relatively small size of multi-junction solar cells which is clearly distinguishable from the standard flat-plate photovoltaic (PV) system available in the market. Moreover, both the cooling system and 2 axis sun-tracking (ST) mechanism is absolutely necessary to attain full potential of electrical power generation in CPV systems (Abdallah, 2004). Overall, 2 axis ST mechanism can be classified into two common types: (1) azimuth-elevation (AE) ST system; (2) tilt-roll (polar) ST system. The AE ST system is one of the most sought-after ST method utilized in various applications as this type of ST system provides maximum collection of solar energy, as stated by Chong and Wong (Chong and Wong, 2008).

An inappropriate layout design of CPV systems in the solar power plant will produce optical losses through mutual shadowing among CPV systems and consequently reduces the electrical power generation. There are various methods that has been carried out by researchers to reduce the effect of mutual shadowing. In 2012, Perpiñán (Perpiñán, 2012) modelled the geometry of mutual shadowing for a square array layout configuration dual-axis ST system. This research made

use of the trigonometry method to determine the minimum separation distance in order to obtain zero-shadowing. Edgar et al. (Edgar, Stachurski and Cochard, 2016) also utilized the trigonometry method to compute the minimum distance between North-South and East-West adjacent rectangular tracking systems for square array layout configuration. Narvarte and Lorenzo (Narvarte and Lorenzo, 2008), Lorenzo et al. (Lorenzo, Narvarte and Muñoz, 2011), Belhachat and Larbes (Belhachat and Larbes, 2015), and, Hu and Yao (Hu and Yao, 2016) also ventures in the geometry modelling of the mutual shadowing for different kinds of ST systems or field geometries. This method is less preferable since it can only be utilized for zero-shadowing condition which leads to an increase in the utilization of land area. There is another method by Fartaria and Pereira (Oliveira Fartaria and Collares Pereira, 2013), i.e. ray-tracing method, at which this method determines the losses due to shadowing for direct normal irradiance (DNI) in both square array and staggered array layout of the solar dish field. Dähler et al. (Dähler, Ambrosetti and Steinfeld, 2017) also produced a simulation model in 2017 using the ray-tracing method under two assumptions, i.e. the sunrays are parallel and the sun tracking is perfect. This assumption was set so as to find the shading efficiency of the solar dish field with respect to ground-cover ratio (GCR). Their study assume that the whole tile is fully shaded provided that the central point of the tile is shaded. Although this method provides accurate results, it needs a long computational time. This computational time of ray-tracing method can be reduced significantly by using a special algorithm which utilize the ray/plane algorithm (four-point method), developed by Chong and Tan (Chong and Tan, 2012). Their study used this algorithm to

determine both the effect of shadowing and blocking for heliostat field in central tower system.

There are different ways on how researchers optimize the performance of large solar power plant. In 2014, factors such as layout combinations of aspect ratio, offset and ground-cover-ratio in the optimization of solar collector position has been considered in a research conducted by Cumpston and Pye (Cumpston and Pye, 2014) to reduce the annual shading for a range of collector densities based on their case study in Barstow, California. They also assumed that all of the nearby sites are occupied. Therefore, the simulation of the array edge effects is not performed in their study. Based on the study conducted by Pons and Dugan (Pons and Dugan, 1984), they clearly expressed that the edge effect can be neglected in a square or near-square array layout configurations provided that the layout configurations had more than 50 collectors. The research groups that have neglected this edge or border effects in their studies include Edwards (Edwards, 1978), Gordon and Wenger (Gordon and Wenger, 1991), and Meller and Kribus (Meller and Kribus, 2013). It is predicted by Dähler et al. (Dähler, Ambrosetti and Steinfeld, 2017) in 2017 that the optical performance of a solar dish field can be optimized in terms of shading efficiencies and ground-cover ratio. They also specified that the border effect is excluded in their study since this effect is assumed to be less important with increasing field size.

The levelized cost of electricity (LCOE) has been one of the essential ways to evaluate the economic feasibility of photovoltaic projects when the solar energy technologies become more mature and competitive. This enables it to compare with the cost of other technologies in electricity generation plant. The LCOE is an assessment parameter to evaluate the economic aspect of a power

generation plant. According to the previous works, the optimization of PV field layout design only comes with the consideration of the system performance by reducing or eliminating the mutual shadowing amid the PV system. The LCOE of the solar PV systems must be reduced significantly to garner possible investors to invest in solar power installations but there is currently no existing study yet to be done on the LCOE optimization of the CPV field layout using the actual meteorological data.

Here, a new computational algorithm is proposed to optimize the LCOE of the field layout design accordingly to the local meteorological data. It is significant to reduce the mutual shadowing by increasing the separation distance between adjacent CPV systems in the field but this idea incurs more utilization of land area, which led to an increase in land-related costs. The separation among adjacent CPV systems is a trade-off between land utilization and productivity in which it is of utmost importance to optimize the economic balance between land cost and the output of power generation.

1.1 Problem statement and research objectives

The CPV with dual-axis sun-tracking system is needed to achieve the maximum production of solar energy. However, the inappropriate CPV module allocation plan in solar field will generate optical losses caused by mutual shadowing between CPV module arrays that contributes to the reduction of electrical energy. Presently, there is no such study in Malaysia and overseas that have performed the optimization process of field layout based on the levelized cost of electricity (LCOE) using local weather data. The newly proposed computational algorithms

can evaluate the performance of a dual-axis sun-tracking method and optimize the land usage of the CPV module field layout accordingly. This research will benefit our society significantly as it may help improve our technologies to tap more renewable energy efficiently. The objectives of this research work are as follow:

- a) To develop a computational algorithm to simulate the mutual shadowing between dual-axis CPV sun-tracking system at various field layout design.
- b) To evaluate the shadowing effect on a dual-axis CPV sun-tracking system by considering various field layout designs.
- c) To determine the optimal field layout design for a dual-axis CPV sun-tracking system in a solar field by considering the shadowing effect and actual meteorological data based on the levelized cost of solar electricity (LCOE).

1.2 Scope of research

This research presented a new computational algorithm to optimize the LCOE of the field layout design based on the local meteorological data, geographical location of the site (latitude and longitude), specification of CPV system, land aspect ratio of CPV farm, shadowing efficiency, edge effect, the spacing of adjacent CPV systems, and land cost. The new computational algorithm had been developed and implemented using the MATLAB simulation software. This research provided a methodology which can be applied to assist researchers and engineer to optimize the field layout design of the CPV systems in order to achieve the lowest possible investment in term of LCOE.

1.3 Outline of thesis

The structure of the thesis is presented as follows:

- Chapter 1 introduced the research background and the existing problems under study.
- Chapter 2 reviewed the past research works that are related directly and indirectly to the preliminary of this research.
- Chapter 3 described an outline of the methodology used in this research. In this research, the simulation algorithm was modelled into two different layout configurations of CPV field: (1) square array configurations; (2) staggered array configurations. The newly developed algorithms were specially tailored to analyze and optimize the solar farm layout, which consisted of CPV systems that are equipped with dual-axis sun-tracking mechanisms. This methodology can aid researchers and engineer to optimize the field layout design of the CPV systems in order to find the lowest possible investment in terms of LCOE.
- Chapter 4 presented the optimization studies for both the square array and staggered array layouts that have been carried out in a city located in the north of Borneo Island, Kota Kinabalu Malaysia, by taking into account of local meteorological data, shadowing efficiency, annual energy yield, LCOE, land leasing cost, land aspect ratio (LAR), and the edge effect.
- Chapter 5 concluded the overall research and recommended future work will be elaborated.

CHAPTER 2

LITERATURE REVIEW

The effect of global warming issues give rise to the increasing concern of looking for another possible sources of energy, i.e. safe, clean and renewable. The increasing amount of interest in the photovoltaic (PV) and concentrator photovoltaic (CPV) systems are caused by the invention of solar cells and their continuous development on improved efficiency (Green *et al.*, 2016; Tan and Chong, 2016). Conversion of the sun's energy into electrical energy can be done by using the photovoltaic (PV) system as it is one of the natural resources which are clean, renewable as well as abundant in most parts of the world (Eke and Senturk, 2012). In the industry of solar energy, one of the important parameters to determine the effectiveness of a large solar in terms of cost is levelized cost of electricity (LCOE). LCOE is described as the cost per unit energy produced over the entire life of the system. LCOE has to be reduced with the purpose of introducing the solar energy as the main power generation in near future. One of the plans to bring down the LCOE is to increase the power generated by the PV/CPV system.

2.1 Importance of sun-tracking (ST) system

The studies on some of the available types of sun-tracking (ST) system in the world are mentioned and explained in this section. This section also covers the

important basic parameters needed for computation of sun position before applying the relevant values into the general sun-tracking formula (GF) to find out the elevation angle and azimuth angle. Such literature review on this was needed as a base knowledge to be implemented into the codes for the simulations of this research.

Solar power technology is part of the popular renewable energy technology as it has the potential to produce electrical energy and at the same time being pollutant-free and reliable. It can perform well at a very low maintenance costs and has minimal effect on the ecological system (Amarjeet, 2013). There is a variety of solar power technology used for solar energy applications, e.g. solar photovoltaic and solar water heating technology (National Renewable Energy Laboratory, no date).

ST system will be the prime growth factor in the applications of solar energy. The fixed solar panels without the ST system is unable to bring out the maximal energy. Therefore, this development of the ST system is essential to increase the conversion efficiency of solar panels to produce maximum output. This method is feasible by frequently adjusting the orientation of the solar panels towards sun at the optimum angles (Sreekanth, 2011).

A fine ST system must have a good reliability and a great ability to detect the position of the sun accurately at all times even if there is an occasional unpredictable obstacle that may sometimes block some of the sunlight. Nowadays, it is of utmost importance to track the sun position as accurately as possible to extract the maximum output from the solar collector. Hence, the

general sun-tracking formula (GF) was introduced and derived to enable the ST system to function efficiently (Chong and Wong, 2010).

A universal ST controller for either single or dual axis solar tracker can be designed to accurately pin-point and adjust the angles of the solar collector by applying the GF into the system. The GF can give us an overall mathematical idea to calculate the sun position which can be easily simulated by using Microsoft Excel. Besides, it helps to increase the precision of ST system through the compensation of the solar collector's installation error. This can be done without much difficulty by changing the value of three main parameters in the GF (Chong and Wong, 2010). This is definitely one of the best methods to see an exceptional increase in the ST accuracy.

2.1.1 Types of sun-tracking (ST) system

Before starting the project, there is a need to at least have a basic idea of the distinct variety of sun-tracking (ST) system available in the world. The ST systems are divided into two different groups, i.e. single-axis (1 axis) ST system and dual-axis (2 axis) ST system. The Figure 2.1 represents the types of ST system available in the world.

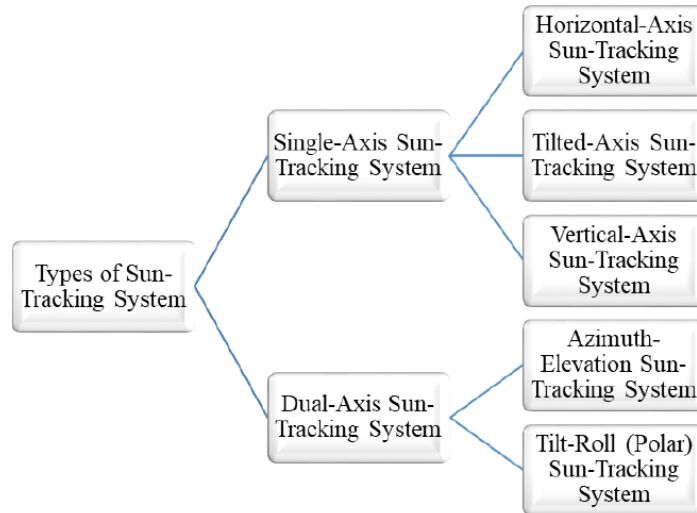


Figure 2.1: Types of available sun-tracking (ST) system.

2.1.2 1 axis sun-tracking (ST) system

A 1 axis sun-tracking (ST) systems fundamentally rotate on one axis following the motion of the sun in one direction, i.e. North-South or East-West (Pérez-Higueras *et al.*, 2015). In general, each type of 1-axis ST system contains the following basic characteristics as stated in Table 2.1. Besides, the examples of 1 axis ST systems are shown in Figure 2.2 and Figure 2.3.

Table 2.1: Basic characteristics of each type of 1 axis sun-tracking (ST) system

1 Axis ST System	Basic Characteristics
Horizontal-Axis ST System	<ul style="list-style-type: none"> • ST axis is aligned with the earth's surface. It can be placed either along North-South (NS) or East-West (EW) direction. • It is usually used for areas near the equator where the sun's position during noon time is at its highest (Johnson-Hoyte <i>et al.</i>, no date).

Tilted-Axis ST System	<ul style="list-style-type: none"> • ST axis is tilted, i.e. neither vertical nor horizontal. • The major benefit of this type of ST system is that it can be densely placed together in a limited area. • This particular system almost reaches the performance of a 2 axis ST system (U.S. Department of Energy, 2014).
Vertical-Axis ST System	<ul style="list-style-type: none"> • ST axis is aligned with zenith axis. • Mostly recognized as Azimuth ST system. • This type of ST system usually used at places with high latitude as the sun's position do not get as high during noon (Johnson-Hoyte <i>et al.</i>, no date).



Figure 2.2: Applications of 1 axis sun-tracking (ST) system for solar PV panel
(Rockwell Automation, 2011)



Figure 2.3: Applications of 1 axis sun-tracking (ST) system for solar thermal parabolic trough (Rockwell Automation, 2011)

2.1.3 2 axis sun-tracking (ST) system

The maximum efficiency of energy collection can be done by utilizing a 2 axis sun-tracking (ST) system which follows the sun's movement both vertically and horizontally (Zip, 2013). Typically, some examples on 2 axis ST system and its basic characteristic explained in Table 2.2. There are also examples of 2 axis ST systems shown in Figure 2.4 and Figure 2.5.

Table 2.2: Basic characteristics of each type of 2 axis sun-tracking system

1 Axis ST System	Basic Characteristics
Azimuth-Elevation (AE) ST System	<ul style="list-style-type: none"> • This ST system ought to be able to revolve freely around both azimuth and elevation axes. • The azimuth axis of the sun-tracking system has to be aligned to the zenith axis.

	<ul style="list-style-type: none"> • The elevation axis must be 90 degrees from the azimuth axis. It is also aligned to the surface of the earth. • Applicable to large and heavy solar panels (D. Nagesh, M. Ramesh, 2015)
Tilt-Roll (Polar) ST System	<ul style="list-style-type: none"> • The main operation of this ST system is that it changes the tilt angle based on the sun path. • Besides, it also follows the motion of the sun from the East to the West daily. • One of the axes in the Polar ST system is that it is placed with alignment to the polar axis of our Earth which is pointed directly to the Polaris star. • Therefore, the sun collector of this ST system is indirectly tilted and the tilted angle is equal to the latitude angle of a specific location (D. Nagesh, M. Ramesh, 2015).



Figure 2.4: Applications of 2 axis sun-tracking (ST) system for solar PV panel
(Rockwell Automation, 2011)



Figure 2.5 Applications of 2 axis sun-tracking (ST) system for solar thermal dish (Rockwell Automation, 2011)

2.1.4 Justification of both the sun-tracking (ST) system

2 axis sun-tracking (ST) systems uses both motion along the elevation axis and azimuth axis. This type of ST system actually gives the best performances since it follows the motion of the sun accurately unlike 1 axis ST system (Swetansh, 2013). Therefore, the further comparison between both of the ST systems are tabulated in Table 2.3. Based on the comparison, it can be concluded that each type of ST system has its own good and bad points. However, each type can be better than the other for different types of solar energy applications.

Table 2.3: Comparison between both sun-tracking (ST) systems (solarflexrack, 2013)

Components	1 axis ST system	2 axis ST system
Cost	Low	High
Reliability	High	Low
Life span	Long	Short
Energy output during sunny days	Low	High
Flexibility	Low	High
Accuracy	Low	High
Complexity	Simple	Complex

2.1.5 Basic computations of sun position

According to Lovegrove et al. (Lovegrove *et al.*, 2013), they mentioned that we can roughly calculate the sun's position with respect to the solar collector. In their studies, they stated the simple equations which helps to estimate the respective position of the sun and the solar collectors based on fixed locations and conditions. The following main parameters such as declination angle, equation of time (EOT), local clock time (LCT) and hour angle are needed for calculation before applying them into the GF.

The declination angle, δ is well known as an angle that measures from the line to the sun to the equatorial plane of the earth. Based on Figure 2.1, it can be seen that the declination angle changes throughout the year. In order to calculate the declination angle, the following equation is applied (Lovegrove *et al.*, 2013).

$$\delta = \sin^{-1}\{0.39795 \cos[0.98563(N - 1)]\} \text{ (degrees)} \quad (2.1)$$

where δ = declination angle and N = day number of the year.

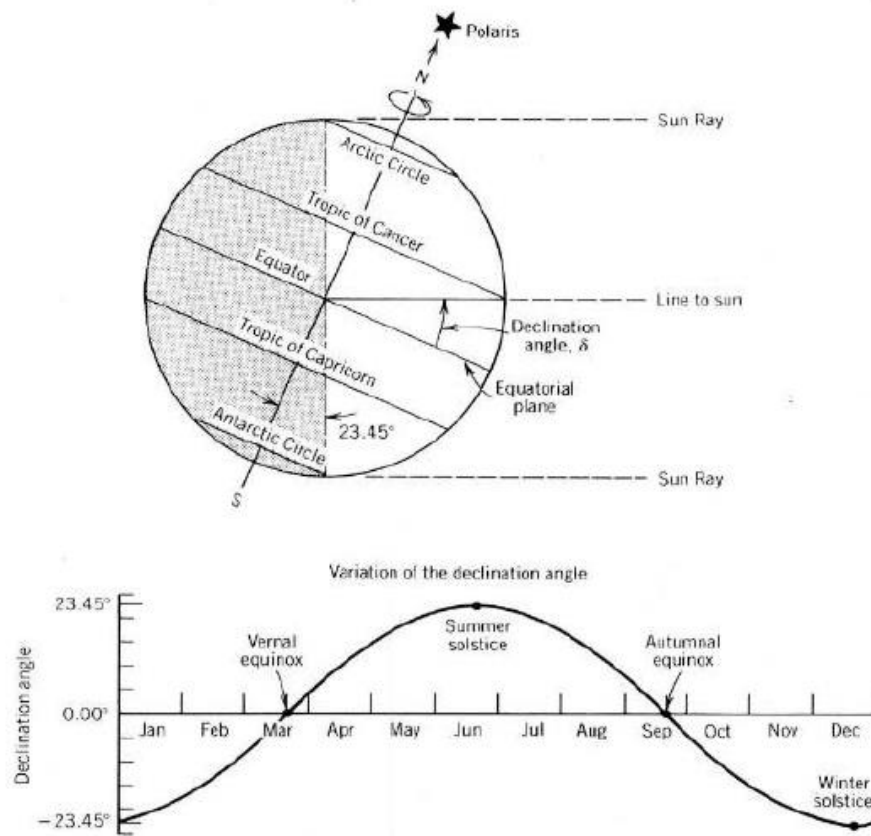


Figure 2.6: The variations of declination angle throughout the year (Lovegrove *et al.*, 2013)

The equation of time (EOT) computation mentioned by Lovegrove *et al.* (Lovegrove *et al.*, 2013), the Eqn. 2.2a and 2.2b are applied.

$$\text{EOT} = 0.258 \cos x - 7.416 \sin x - 3.648 \cos 2x - 9.228 \sin 2x \quad (2.2a)$$

(min)

where x = function of the day, N

$$\chi = \frac{360(N-1)}{365.242} \text{ (degrees)} \quad (2.2b)$$

Local clock time (LCT) represents the time at a specific location. Normally, the LCT can be utilized to compute the solar time of the particular location. Solar time is basically expressed in 24 hours with 12:00 as a point which the sun reaches its highest position in the sky. The solar time varies depending on the longitude of a particular location (Honsberg, 2015). The equations used are as shown below (Lovegrove *et al.*, 2013):

$$LCT = t_s - \frac{EOT}{60} + LC + D \text{ (hours)} \quad (2.3a)$$

where

$$LC = \frac{\text{Longitude of Standard Time Zone} - \text{Local Longitude}}{15} \text{ (hours)} \quad (2.3b)$$

D = daylight savings time in hours (if in effect, D=1, otherwise D=0).

In Malaysia, the longitude of standard time zone is 120 degrees. This is because we are located at GMT+8. Therefore, longitude of standard time zone = 8 x 15 degrees = 120 degrees. Besides, D is equal to 0 in Malaysia, since there is no daylight savings time in effect.

The hour angle, ω , basically describes the difference between the time of the current day and its solar noon (Dawson, 2013). The value of hour angle is 0 degrees at solar noon and it will increase or decrease by 15 degrees every hour

accordingly to the time of day. The hour angle can be calculated using the following equation (Lovegrove *et al.*, 2013):

$$\omega = 15(t_s - 12) \quad (\text{degrees}) \quad (2.4)$$

where t_s = solar time in hours.

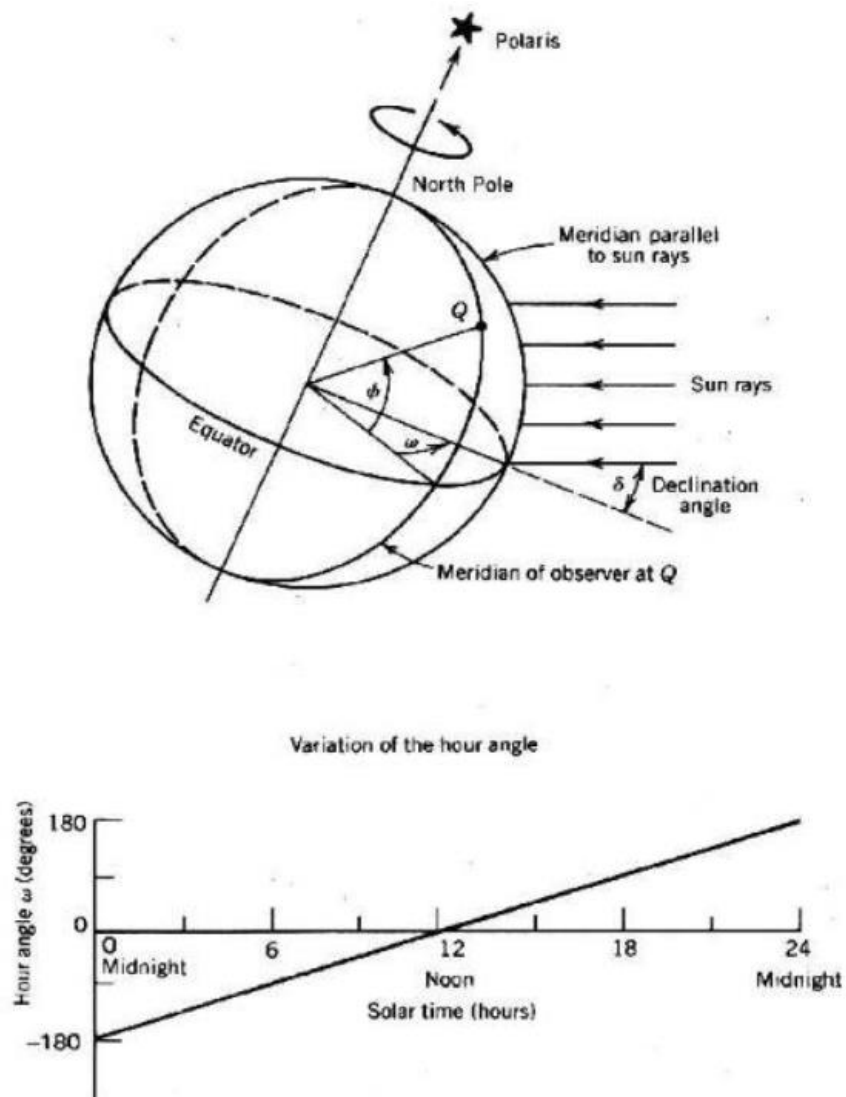


Figure 2.7: The variations of hour angle throughout the day (Lovegrove *et al.*, 2013).

In the earlier part of Section 2.1, it is mentioned that the GF can help to increase the accuracy of any type of ST system either 1 axis (e.g. polar ST system) or 2 axis ST system (e.g. azimuth-elevation ST system). According to Chong and Wong (Chong and Wong, 2010), the calculations or computations of the sun position can be done by setting the 3 important parameters and apply relevant values into the respective equations derived by them. These knowledges obtained from this paper was applied into the fundamental codes in this research study.

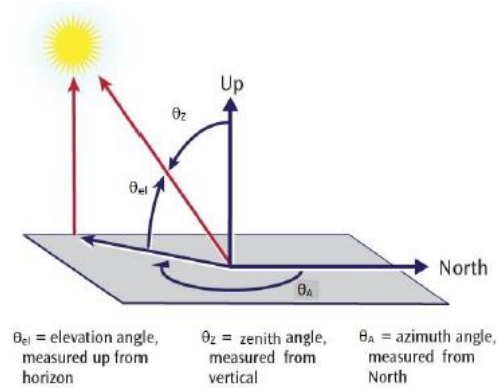


Figure 2.8: Position of elevation angle, α and azimuth angle, β
(PVPerformance Modeling collaborative, no date)

2.2 Overall review of the electrical performance of PV/CPV system

In order to enhance the overall electrical performance of the PV/CPV systems, scientist and researchers have studied the ST systems in various ways. According to Mousazadeh et al. (Mousazadeh *et al.*, 2009), the electrical power generation of single-axis tracking PV system will increase by 24.5% as compared to fixed-mounted PV system. In Jordan, Abdallah has performed an overall study on the generation of electrical power of the different categories of PV system (Abdallah,

2004). He outlined that the electrical power generation of 2 axis tracking PV system performed an improvement of 43.87% than that of fixed-mounted PV system which had an inclination of 32° facing the south. According to the report made by Gomez-Gil et al. (Gómez-Gil, Wang and Barnett, 2012), the energy generation for 1 axis are 22.3% more in the annual energy generation analysis than that of the fixed flat plate system whereas the 2 axis tracking flat plate systems has 25.2% more as compared to the than that of the fixed flat plate systems. Based on the previously mentioned studies, the ST PV system is deduced to have a great electrical performance improvement than the fixed-mounted PV system.

In 2012, Chong and Tan (Chong and Tan, 2012) had studied the optical losses of heliostat field in their case study by considering the losses, e.g. shadowing effect, caused by the field layout configuration. However, no studies have been done for the optical loss of the dual axis sun-tracking PV system field. In the course of integration with the national grid, the shadowing between PV/CPV module arrays will reduce the electrical energy generation as there will be current mismatch among the solar cells. The mutual shadowing can be reduced by widening the separation between adjacent PV/CPV arrays. However, the method needs more land space and this leads to an increase in land-related costs. Land costs may fall within annual operating and maintenance costs or initial investment, depending on the ownership of the land. Nevertheless, it increases the levelized cost of electricity (LCOE) by great margin, especially when it comes to a utility-scale solar plant which have acres of land. In some countries, the land is a scarce resource and invaluable asset for the nation. Therefore, it must not be wasted under any circumstances.

2.3 Methods/Algorithm used by researchers on layout optimization

The optical losses produced through mutual shadowing among CPV systems due to inappropriate layout design of CPV systems in the solar power plant will consequently reduce the electrical power generation. There are a number of methods that has been used by researchers to minimize the effect of mutual shadowing as shown in the following subsections:

2.3.1 Geometry of mutual shadowing

In 2012, Perpiñán (Perpiñán, 2012) modelled a square array layout configuration dual-axis ST system by using the geometry of mutual shadowing as shown in Figure 2.9 and 2.10. This trigonometry method is applied to determine the minimum separation distance in order to obtain zero-shadowing. Edgar et al. (Edgar, Stachurski and Cochard, 2016) also utilized the trigonometry method to calculate the minimum distance between North-South and East-West adjacent rectangular tracking systems for square array layout configuration. Narvarte and Lorenzo (Narvarte and Lorenzo, 2008), Lorenzo et al. (Lorenzo, Narvarte and Muñoz, 2011), Belhachat and Larbes (Belhachat and Larbes, 2015), and, Hu and Yao (Hu and Yao, 2016) also partake in the geometry modelling of the mutual shadowing for several kinds of ST systems or field geometries. This method is less preferable since it can only be used for zero-shadowing condition where it will lead to an increase in the area of land utilization.

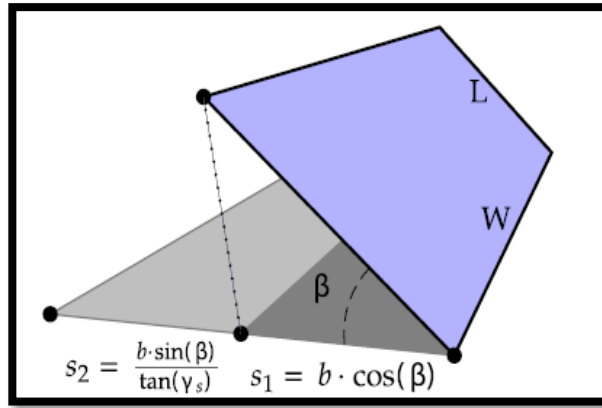


Figure 2.9 (a): Dimensions of a 2 axis tracker and length of its shadow.

(Perpiñán, 2012)

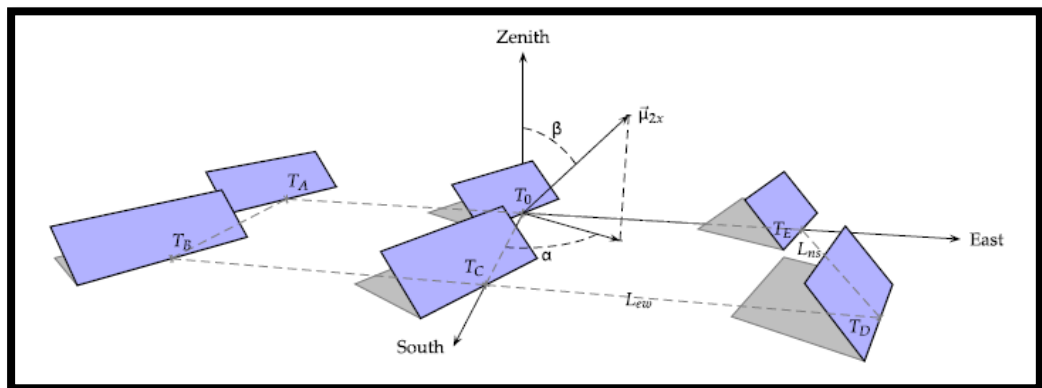


Figure 2.9 (b): Mutual shadowing effect between six 2 ST system.

(Perpiñán, 2012)

2.3.2 Ray-tracing (point-to-point) method

There is another method introduced by Fartaria and Pereira (Oliveira Fartaria and Collares Pereira, 2013), i.e. ray-tracing method, which is also known to be “point-to-point” method. This method helps to determine the losses occurred due

to shadowing for direct normal irradiance (DNI) in both square array and staggered array layout of the solar dish field.

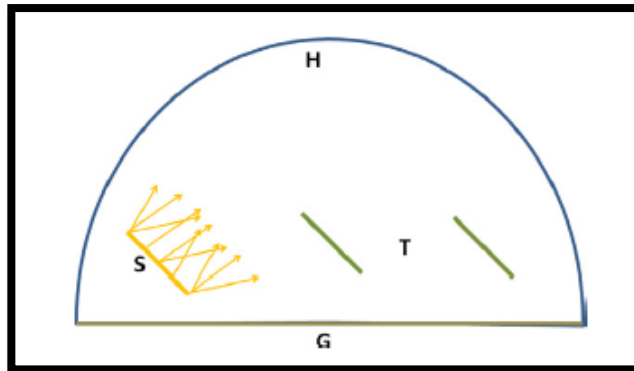


Figure 2.10: Ray-tracing method for shadow loss, where H is the horizon (represented by a sphere), G is the ground, S is the isotropic rectangular source and T are the sun tracking system that will shade the source. (Oliveira Fartaria and Collares Pereira, 2013)

Other than Fartaria and Pereira, Dähler et al. (Dähler, Ambrosetti and Steinfeld, 2017) also made a simulation model in 2017 by utilizing the ray-tracing method under two assumptions, i.e. the sunrays are parallel and the sun tracking is perfect. This assumption was set in order to find the shading efficiency of the solar dish field with respect to ground-cover ratio (GCR). In their study, it is assumed that the whole tile is completely shaded provided as long as the central point of the tile is shaded. However, this method needs a long computational time although the results are accurate.

2.3.3 Ray/Plane algorithm (Four-point method)

A special algorithm can be used to reduce the computational time of ray-tracing method significantly. This algorithm utilized the ray/plane algorithm (four-point method), developed by Chong and Tan (Chong and Tan, 2012). Their study used this algorithm to determine both the effect of shadowing and blocking for heliostat field in central tower system. This study assumes that the path of sunlight is straight. Computational time is reduced but the study is only based on heliostat field.

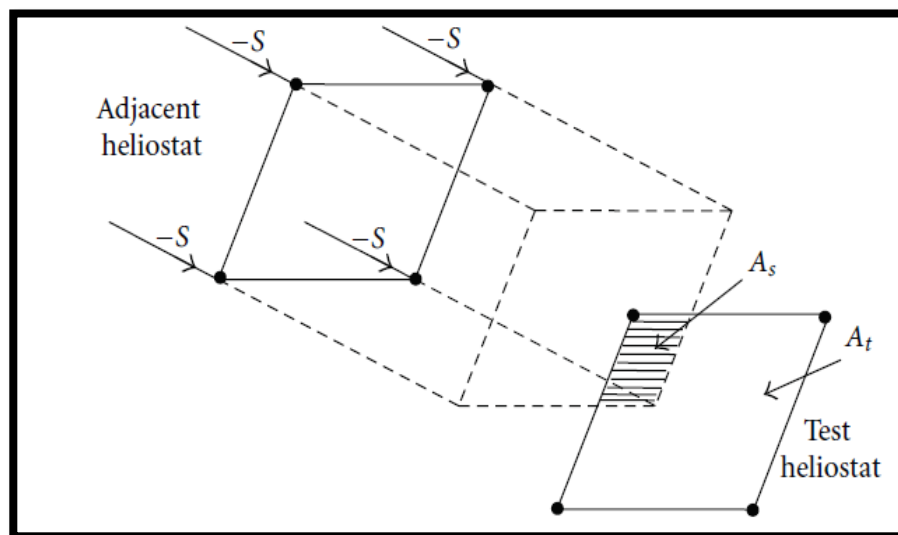


Figure 2.11: Shadowing effect on "Test Heliostat". (Chong and Tan, 2012)

2.4 Research approach in the optimization of large solar power plant

There are different means on how researchers optimize the performance of large solar power plant. It is normal for researchers to consider factors such as layout combinations of aspect ratio, offset and ground-cover-ratio in the optimization

of solar collector position. However, none of them considered to include edge effects into their studies.

In 2014, factors such as layout combinations of aspect ratio, offset and ground-cover-ratio in the optimization of solar collector position has been considered in a research performed by Cumpston and Pye (Cumpston and Pye, 2014) to reduce the annual shading for a range of collector densities of their research in Barstow, California. They also assumed that all of the nearby sites are occupied. Therefore, the simulation of the array edge effects is not performed in their study. Based on the study conducted by Pons and Dugan (Pons and Dugan, 1984), they mentioned that the edge effect can be neglected in a square or near-square array layout configurations provided that the layout configurations had more than 50 collectors.

The many other research groups have neglected this edge or border effects in their studies. They were Edwards (Edwards, 1978), Gordon and Wenger (Gordon and Wenger, 1991), and Meller and Kribus (Meller and Kribus, 2013). In 2017, it is predicted by Dähler et al. (Dähler, Ambrosetti and Steinfeld, 2017) that the optical performance of a solar dish field can be optimized in terms of shading efficiencies and ground-cover ratio. Besides, they also mentioned that the border effect is excluded in their study since this effect is assumed to be less important with increasing field size.

2.5 Levelized cost of electricity (LCOE)

The levelized cost of electricity (LCOE) has always been one of the essential ways to evaluate the economic feasibility of photovoltaic projects when the solar

energy technologies become more mature and competitive. This enables it to compare with the cost of other technologies in electricity generation plant. The LCOE is an assessment parameter to evaluate the economic aspect of a power generation plant. According to the previous work done by other researchers, the optimization of PV field layout design only comes with the consideration of the system performance by reducing or eliminating the mutual shadowing amid the PV system. The LCOE of the solar PV systems must be reduced significantly to attract possible investors to invest in solar power installations but there is currently no existing study yet to be done on the LCOE optimization of the CPV field layout using the actual meteorological data.

In this research, a new computational algorithm is proposed to optimize the LCOE of the field layout design accordingly to the local meteorological data. It is significant to reduce the mutual shadowing by increasing the separation distance between adjacent CPV systems in the field but this idea causes more utilization of land area and this led to an increase in land-related costs. The separation among adjacent CPV systems is a trade-off between land utilization and productivity in which it is of utmost importance to optimize the economic balance between land cost and the output of power generation.

CHAPTER 3

METHODOLOGY

A newly proposed computational algorithm has been developed and implemented using the MATLAB simulation platform. The algorithm of this simulation can be modelled into two different types of CPV layout configurations in solar CPV field, i.e. square array and staggered array configurations, by considering the annual local meteorological data, land aspect ratio, edge effect, and the spacing of adjacent CPV systems. The methodologies of the simulation algorithm to optimize both the square array and staggered array layout configurations are detailly shown in Figure 3.1 and Figure 3.2 respectively. The newly developed algorithms were specifically customized to analyze and optimize the dual-axis sun-tracking CPV system for solar farm layout configurations by perform the following actions: (a) computing annual shadowing effect and annual energy generation of the different layout configurations, (b) optimizing the LCOE of both layout configurations. The relative positions of adjacent CPV systems in a solar farm is varied to compute the optimization of field layout configuration. Here, the trade-off between land utilization and productivity can be observed clearly in this research study. Thus, the study of the economical balance between land-related cost and cost of electricity generation is done using the simulated results. The methodology of this research study has also been submitted, accepted and published in Solar Energy Journal May 2020 as shown in Appendix B.

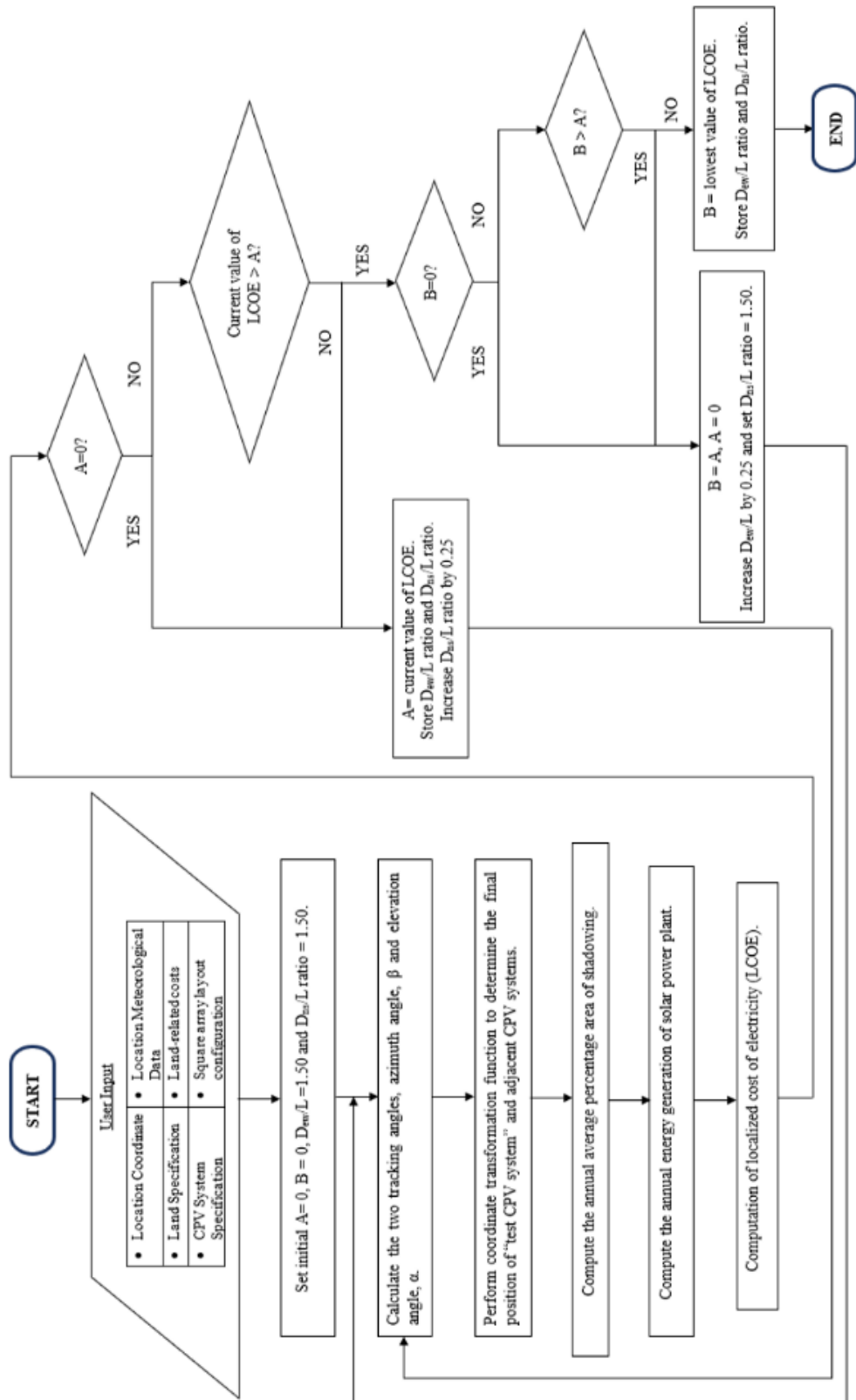


Figure 3.1: Methodology of computational algorithm for optimizing the square array layout configuration.

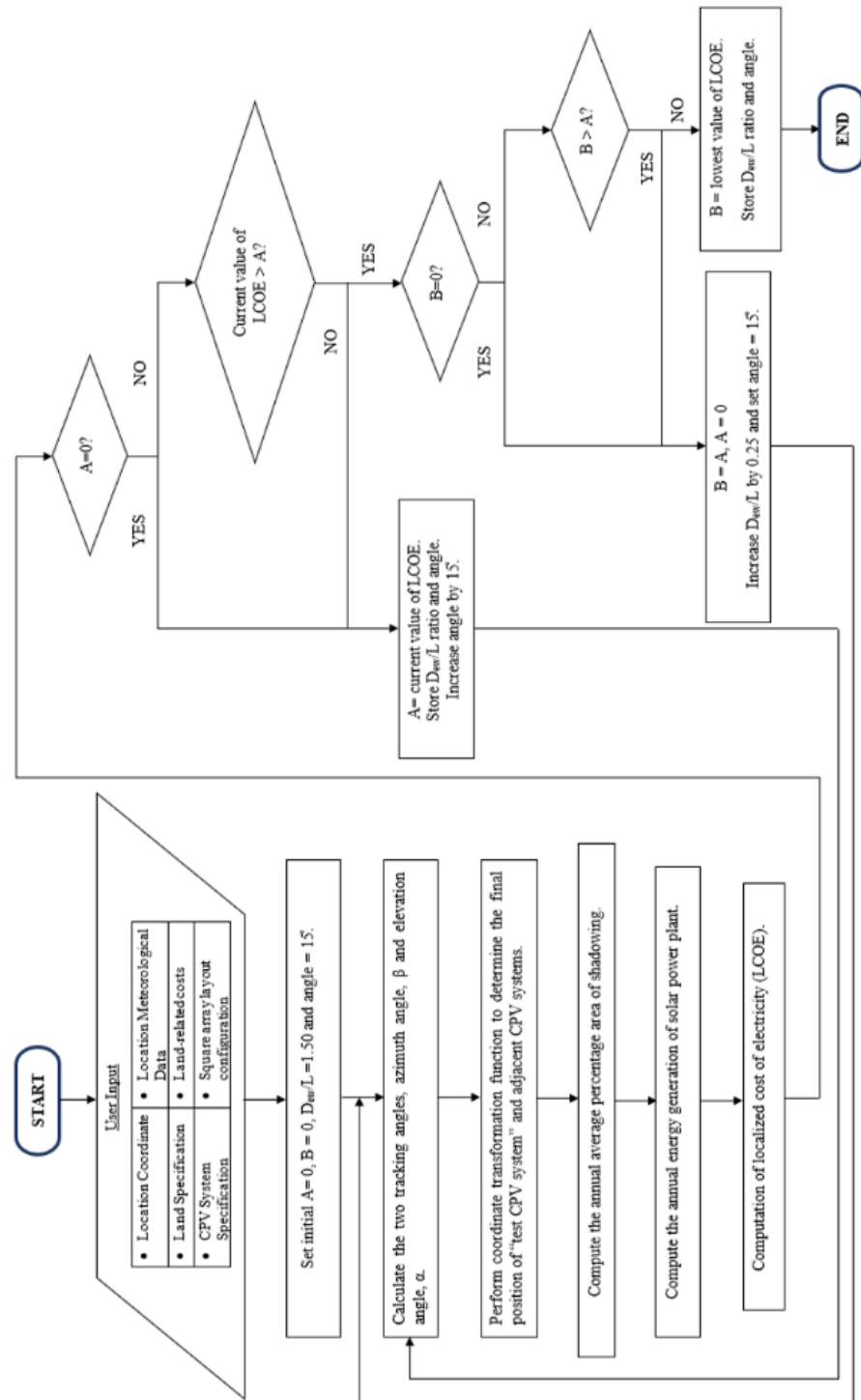


Figure 3.2: Methodology of computational algorithm for optimizing the staggered array layout configuration of CPV field in MATLAB simulation platform.

3.1 Sun-tracking (ST) angles

The dual-axis ST mechanism is important to precisely track the sun position and to gain the maximum possible power conversion for the CPV system as the sun position changes accordingly throughout the day and year. In this research study, the most common ST method is proposed in this study. Chong and Wong (Chong and Wong, 2008) specified that the two ST angles of Azimuth-Elevation ST method, i.e. elevation angle, α and azimuth angle, β , can be acquired from the general sun-tracking formula (GF) by setting the three orientation angles of solar collector to zero as expressed in the following equations:

$$\alpha = \sin^{-1}(\sin \delta \sin \Phi + \cos \delta \cos \omega \cos \Phi) \quad (3.1a)$$

$$\beta = \cos^{-1}\left(\frac{\sin \delta \cos \Phi - \cos \delta \cos \omega \sin \Phi}{\cos \alpha}\right) \quad (3.1b)$$

where δ is the sun declination angle, ω is the hour angle, Φ is the latitude.

If $\sin \omega > 0$, then $\beta = 2\pi - \beta$.

3.2 Coordinate transformation

The coordinate transformation method is used in this research study to model how each individual CPV system, e.g. point-focus Fresnel lens CPV system (Figure 3.3), installed on sun-tracker while performing sun-tracking. Firstly, there is a need to identify the orientations of the individual CPV system to determine the effect of shadowing between adjacent CPV systems. The

modelling of three-dimensional (3-D) space for the instantaneous CPV systems position during the daily operation of sun-tracking can be accomplished through the coordinate transformation. Another one-dimensional (1-D) space has been added into the existing coordinate transformation in order to ease the 3-D coordinate transformation by performing linearization.

In order to proceed into the coordination transformation, the origin of the global coordinate system, $\mathbf{O}(0,0,0)$ is defined at the central point of the CPV field as shown in Fig. 5 in which the positive X-axis direction, x , points towards east (E); the positive Y-axis direction, y , points towards north (N); and the positive Z-axis direction, z , points towards zenith where zenith is the direction opposite of the gravitational pull. The initial coordinate of the individual CPV system is assumed to be set in a local coordinate system as depicted in Fig. 4, where the local origin, $\mathbf{C}(0,0,0)$, is located at the center of structural frame of the CPV system instead of the central point of the CPV field. There are four corners of the CPV system at which each corner is represented by an edge point. The coordinates of the four edge points in the coordinate space are set as a vector. This can be represented by the equation below:

$$\mathbf{P}_k = \begin{bmatrix} \mathbf{P}_{kx} \\ \mathbf{P}_{ky} \\ \mathbf{P}_{kz} \\ 1 \end{bmatrix} \quad (3.2a)$$

where $k=1$ (for top left, TL, corner of structural frame of the CPV system), $k=2$ (for top right, TR, corner of structural frame of the CPV system), $k=3$ (for bottom right, BR, corner of structural frame of the CPV system), and $k=4$ (for bottom left, BL, corner of structural frame of the CPV system).

The final coordinate transformation of the edge points is represented as a vector in the form of matrix as shown in Eqn. 3.2b after performing the coordinate transformation for the structural frame of the CPV system.

$$H_k = \begin{bmatrix} H_{kx} \\ H_{ky} \\ H_{kz} \\ 1 \end{bmatrix} \quad (3.2b)$$

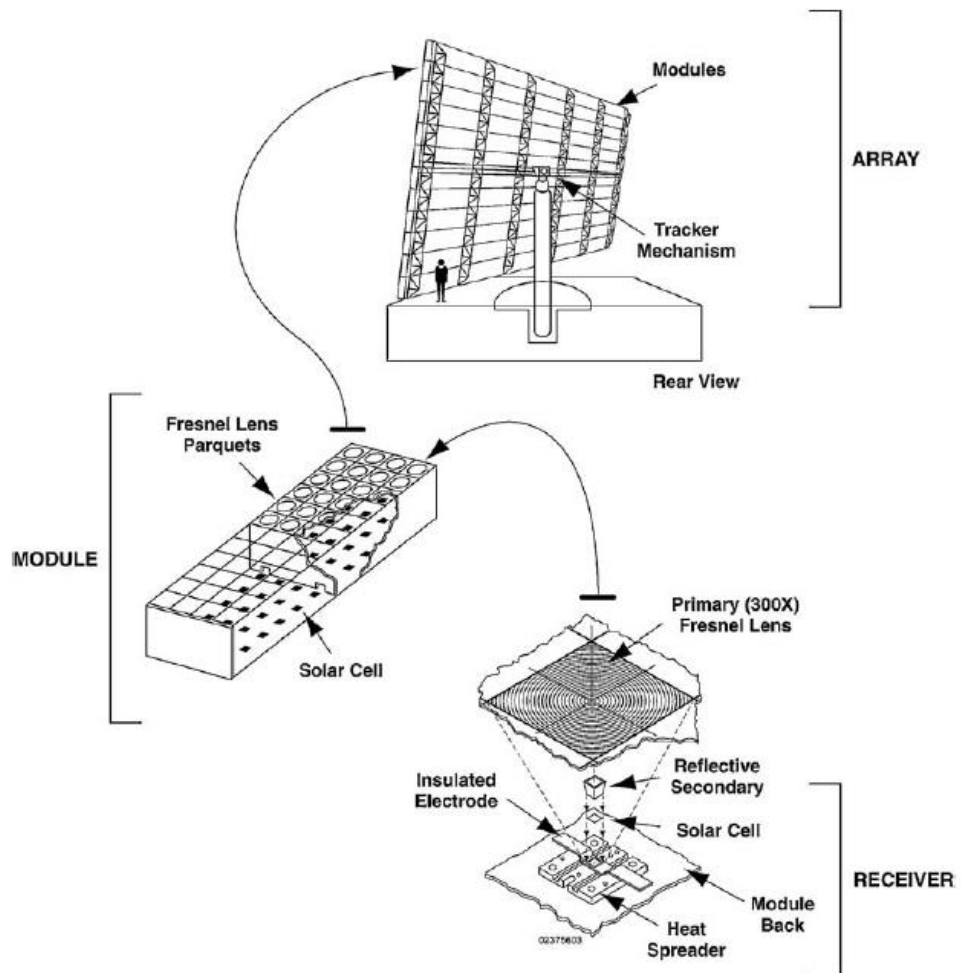


Fig. 3.3. The point-focus Fresnel lens CPV system that is used in the modelling of CPV farm layout (Muñoz *et al.*, 2010)

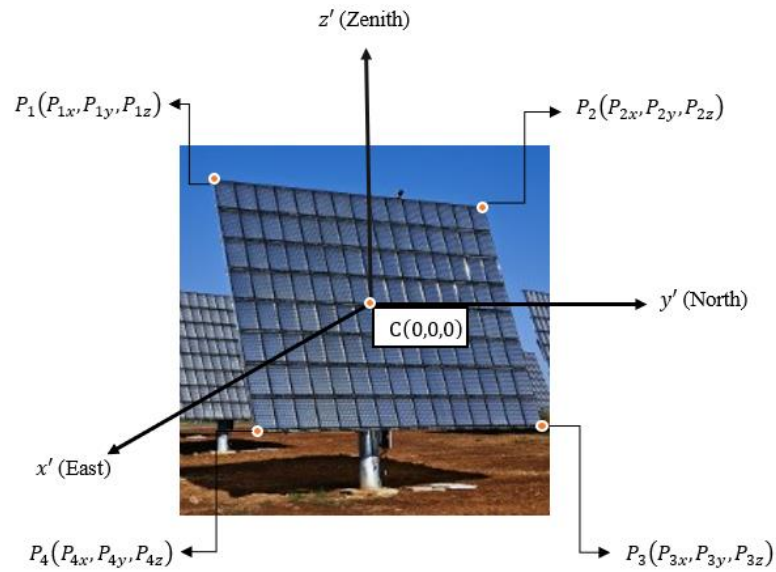


Figure 3.4: The initial coordinate for a structural frame of individual CPV system is defined in a local coordinate system, where the origin is defined at the center of structural frame of the CPV system and P_i is the corner edge point of structural frame of the CPV system.

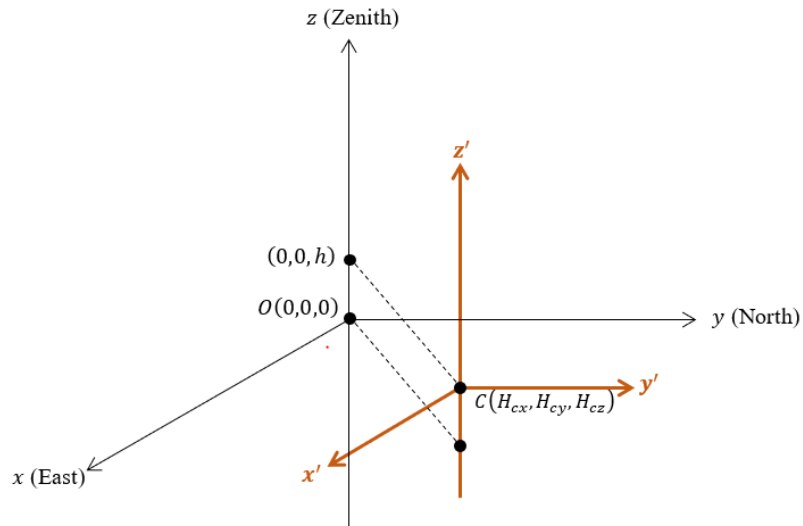


Figure 3.5: The origin, $\mathbf{O}(0,0,0)$, of global coordinate system is defined as the centre of the CPV field. The final coordinate of structural frame of the CPV system is defined as $C(H_{cx}, H_{cy}, H_{cz})$ after performing the coordinate transformation.

The translational transformation matrix in this research study is based on the coordinate of the center of individual CPV system, $C (H_{cx}, H_{cy}, H_{cz})$, expressed in terms of global coordinate system shown in the equation below:

$$T_1 = \begin{bmatrix} 1 & 0 & 0 & H_{cx} \\ 0 & 1 & 0 & H_{cy} \\ 0 & 0 & 1 & H_{cz} \\ 0 & 0 & 0 & 1 \end{bmatrix} \quad (3.3a)$$

For Azimuth-Elevation ST method, there are two parameters which represents two different angle movements of the structural frame of the CPV system, i.e. azimuth movement and elevation movement. In order to transform the position of the CPV system structural frame from the origin of global coordinate system to the final coordinate, a translational transformation method is essential to transform the position using coordinate transformation. The rotational transformation matrix used for the elevation angle, α is

$$[\alpha] = \begin{bmatrix} 1 & 0 & 0 & 0 \\ 0 & \cos \alpha & -\sin \alpha & 0 \\ 0 & \sin \alpha & \cos \alpha & 0 \\ 0 & 0 & 0 & 1 \end{bmatrix} \quad (3.3b)$$

Whereas, the rotational transformation matrix applied for azimuth angle, β is

$$[\beta] = \begin{bmatrix} \cos \beta & \sin \beta & 0 & 0 \\ -\sin \beta & \cos \beta & 0 & 0 \\ 0 & 0 & 1 & 0 \\ 0 & 0 & 0 & 1 \end{bmatrix} \quad (3.3c)$$

The final position of structural frame of CPV system after performing the rotational and translational transformation can be shown as

$$\mathbf{H}_k = \mathbf{M}\mathbf{P}_k \quad (3d)$$

where the matrix for the coordinate transformation is written as

$$\mathbf{M} = [\mathbf{T}_1][\beta][\alpha] \quad (3e)$$

3.3 The Sun-incident ray and ray/plane algorithm

The incident sunrays, \mathbf{S} , is needed in order to determine the shadow casted on the test CPV systems. In 2012, Chong and Tan stated that the incident sunray can be expressed by using the following equation (Chong and Tan, 2012):

$$\mathbf{S} = \begin{bmatrix} S_x \\ S_y \\ S_z \end{bmatrix} \quad (3.4a)$$

$$S_x = \cos \alpha_s \sin \beta_s \quad (3.4b)$$

$$S_y = \cos \alpha_s \cos \beta_s \quad (3.4c)$$

$$S_z = \sin \alpha_s \quad (3.4d)$$

where α_s = solar elevation angle and β_s = solar azimuth angle.

The coordinate transformations are performed for both the adjacent blocking CPV systems (the CPV systems that cast shadow on the test CPV system) and test CPV system (the CPV system that is tested for shadowing effect) after the computation of the ST angles to simulate the instantaneous sun-tracking orientation of both CPV systems. The ray/plane algorithm is then implemented into the MATLAB simulation platform to compute the area of the shadow cast

by the adjacent blocking CPV systems on the surface of test CPV system as illustrated in Figure 3.6.

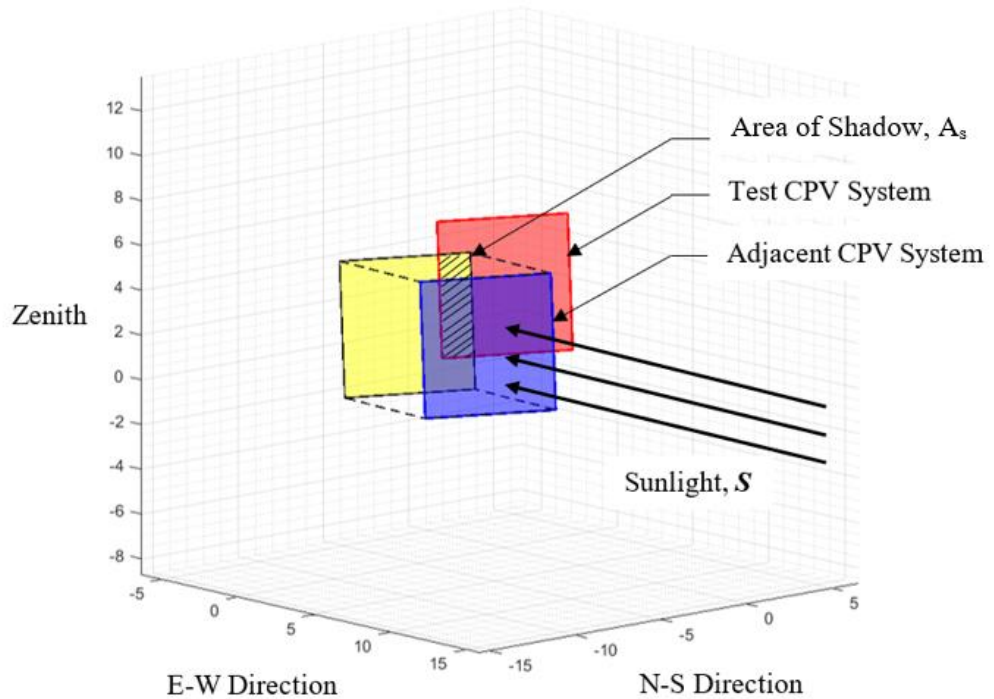


Figure 3.6: Area of shadow caused by adjacent CPV system is computed using the ray/plane algorithm after performing the coordinate transformation for both CPV systems.

3.4 Levelized cost of electricity (LCOE)

The LCOE is a parameter to evaluate the economic aspect of a power generation plant. The economic feasibility study of PV projects is analyzed and assessed according to the LCOE as the solar energy technologies become widely utilized recently. This can provide convenience of comparing with other electricity generation technologies. There are several important factors affecting the LCOE of the solar power plant: (a) local weather data, (b) number of solar concentrators in a specific area of land, (c) total energy produced, (d) land-related costs, and

(e) operational and maintenance cost. According to the review study by Branker et al., they had finalized and presented the Eqn. (3.5) as an appropriate equation to compute the LCOE (Branker, Pathak and Pearce, 2011). The lowest possible computed value of LCOE for the CPV system in solar power plant must be selected to determine the optimized layout design.

$$\text{LCOE} = \frac{\sum_{t=0}^T (I_t + O_t + M_t + F_t)/(1+r)^t}{\sum_{t=0}^T S_t(1-d)^t/(1+r)^t} \quad (3.5)$$

where T is the lifespan of the project in years, t is number of years, I_t is the initial capital cost of the CPV systems including construction, installation, hardware and software of control system etc., M_t is the maintenance costs of the CPV systems for t years, O_t is the operational costs of the CPV systems for t years, F_t is the interest expenditures of the CPV systems for t years, r is the discounted rate of the CPV systems for t years, S_t is the yearly rated energy output of the CPV systems for t years. and d is the degradation rate of the CPV systems.

3.5 Layout configuration

The Figures 3.7 and 3.8 portray two possible layout configurations of CPV field in which all the individual CPV systems are positioned into a square array layout configuration and staggered array layout configuration respectively. These layout configurations of CPV field with the specifications shown in Table 3.1 are used in this case study. The CPV systems for the case study in this research are arranged in either square array or staggered array configuration with different spacing distance within a selected land area of 62,500 m². In order to make a generalization on the spacing distance, D_{ew}/L ratio (the ratio of spacing distance

between the CPV systems in east-west direction to the dimension of a solar collector), D_{ns}/L ratio (the ratio of spacing distance between the CPV systems in north-south direction to the dimension of a solar collector) and spacing angle, θ , have been proposed. The D_{ew}/L ratio and D_{ns}/L ratio can be computed by using the following Eqn. (3.6a) and Eqn. (3.6b). The ground coverage ratio (GCR) has also been implemented into the research as the ratio of the total area of CPV system to the total area of land.

$$D_{ew}/L \text{ ratio} = \frac{\text{Distance between two adjacent CPV systems in east – west direction } (D_{ew})}{\text{Length of CPV system } (L)} \quad (3.6a)$$

$$D_{ns}/L \text{ ratio} = \frac{\text{Distance between two adjacent CPV systems in north – south direction } (D_{ns})}{\text{Length of CPV system } (L)} \quad (3.6b)$$

Table 3.1: Specification of the CPV system solar power plant

Site Location	Kota Kinabalu, Malaysia (Latitude: 5.933°N; Longitude: 116.05°E)
Land area	62,500 m ²
Sun-tracking mechanism	Azimuth-Elevation method
Power conversion efficiency of CPV system	30 %
Degradation rate	0.5%
Dimension of the CPV system	6 m × 6 m = 36 m ²
Height of the CPV system, H _z	4 m

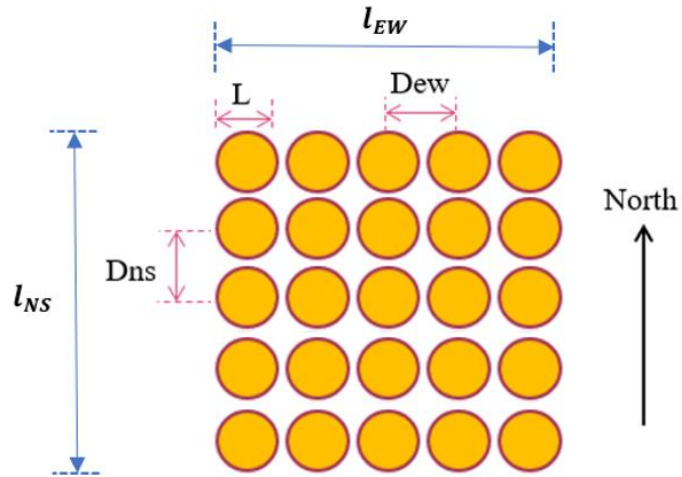


Figure 3.7: Schematic diagram for square array layout of the solar CPV farm.

In the simulation of staggered array layout, the positions of CPV systems in the solar power plant are shown in Figure 3.8. There are a few spacing angles, θ , that are taken into consideration in this case study, i.e. 15 degree, 30 degree, 45 degree, 60 degree and 75 degree.

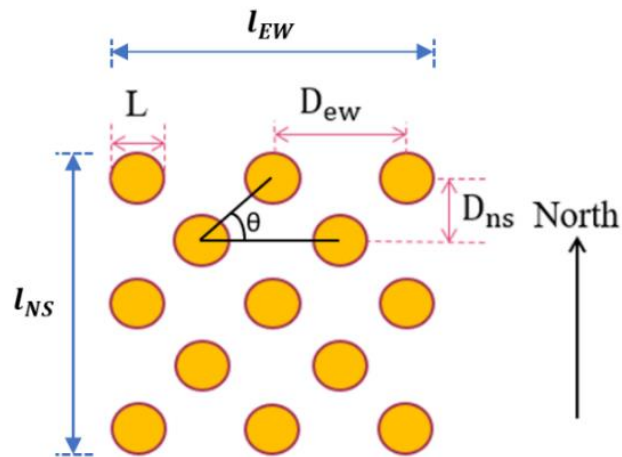


Figure 3.8: Schematic diagram for staggered array layout of the solar CPV farm.

3.6 Annual energy generation

The annual energy generation by the solar power plant needs to be computed in order to calculate the LCOE. The annual energy yield can be calculated using Eqn. (3.7) with the implementation of the local meteorological data, shadowing effect, power conversion efficiency of CPV system, dimension of CPV system and total number of CPV systems in a designated land area. A time interval of 900 seconds (15 minutes) is chosen to attain a more accurate data for a single CPV system.

$$\begin{aligned} & \text{Annual energy (kWh)} \\ & = \sum_{i=1}^{N=365} \sum_{j=1}^{M=96} \frac{\eta \times T \times DNI_{i,j} \times (1 - S_{i,j}) \times A}{3.6 \times 10^6} \end{aligned} \quad (3.7)$$

where i = number of days, j = number of time intervals per day, η is the power conversion efficiency of CPV system, T is the time interval in seconds, DNI is the direct normal irradiance of local sunshine, S is the percentage of collective area affected by shadowing effect and A is the total collector area of each CPV system.

CHAPTER 4

RESULT AND DISCUSSION

A specific land area of 62,500 m² with the land leasing cost of US\$ 12.81/sq. meter has been chosen for this study. The optimization studies for both the square array and staggered array layout configurations have been carried out in a city located in the north of Borneo Island, Kota Kinabalu, Malaysia, by taking into consideration of the local meteorological data, shadowing efficiency, annual energy yield, LCOE, land leasing cost, land aspect ratio (LAR), and the edge effect. The simulation results of this study are further discussed in the following sub-sections.

4.1 Shadowing

The shadow cast on the collective area of CPV system throughout the year is computed at every 15 minutes during the simulation as shown in Eqn. (4.1). For the square array layout configuration, both the D_{ew}/L ratio and D_{ns}/L ratio are varied from the value of 1.50 to 3.00 with an interval of 0.25 to find the optimum distance between two CPV systems. The minimum value of D_{ew}/L ratio and D_{ns}/L ratio are initially set as 1.50, which is the minimum distance required between the two nearest CPV systems to avoid any collision in their sun-tracking trajectories. The total number of CPV systems within the designated land area is dependent on the values of D_{ew}/L ratio and D_{ns}/L ratio.

In order to provide a comparison between square array and staggered array layouts, the simulations of both array layouts were conducted at the same land aspect ratio (LAR), which is $LAR = 1$. The land aspect ratio refers to the ratio of the length of land (l_{EW}) to the width of land (l_{NS}). The staggered array layout is simulated for different D_{ew}/L ratios ranging from 1.5 to 7.0 and different spacing angles θ ranging from 15 to 75 degree. Based on the simulation results obtained on the staggered array layout, the minimum value of D_{ew}/L ratio for each spacing angle is different. This minimum value is set to avoid any possible collision between any two CPV systems. The most possible number of CPV systems to be allocated into the specified land area of 62,500 m² are computed for both the square array and staggered array layout configurations in Table 4.1 and Table 4.2 respectively.

The annual average percentage of collective area that is affected by shadowing effect for the square array and staggered array layouts are shown in Figures 4.1 and 4.2 respectively. Figure 4.1 shows the annual average percentage of shadowing area for square array layout configuration is inversely proportional to both the D_{ew}/L ratio and D_{ns}/L ratio. The simulation result also shows that the spacing distance between any two adjacent CPV systems in east-west (E-W) direction has higher impact of shadowing effect as compared to that of the north-south (N-S) direction. The annual average percentage of shadowing area for staggered array layout configuration has been simulated for different spacing angles as shown in Figure 4.2, which is inversely proportional to the D_{ew}/L ratio. The larger spacing distance between two adjacent CPV systems will have lesser shadowing effect among the CPV systems. However, it is

unfortunate that it causes an increase in the land utilization of the solar power plant which leads to land-related cost.

$$\text{Annual shadowing efficiency, } S_{i,j} = \sum_{i=1}^{N=365} \sum_{j=1}^{M=96} \frac{\eta_s(i,j)}{NM} \quad (4.1)$$

where $\eta_s = \frac{(A_T - A_s)}{A_T}$, η_s is the shadow efficiency, A_T is the area of test CPV system and A_s is the area of shadow.

Table 4.1: The most possible number of CPV systems to be fitted in the designated land area of 62,500 m² for square array layout

D_{ew}/L \ D_{ns}/L	1.50	1.75	2.00	2.25	2.50	2.75	3.00
1.50	729	621	540	486	432	405	351
1.75	621	529	460	414	368	345	299
2.00	540	460	400	360	320	300	260
2.25	486	414	360	324	288	270	234
2.50	432	368	320	288	256	240	208

Table 4.2: The most possible number of CPV systems to be fitted in the designated land area of 62,500 m² for staggered array layout

θ	D_{ew}/L											
	1.50	2.00	2.50	3.00	3.50	4.00	4.50	5.00	5.50	6.00	6.50	7.00
15	C	C	C	C	C	C	C	C	C	357	306	258
30	C	C	C	621	460	368	279					
45	C	718	545	365	265	221						
60	837	492	314	216	161	126						
75	405	226	149	108	81	63						

*C = collided

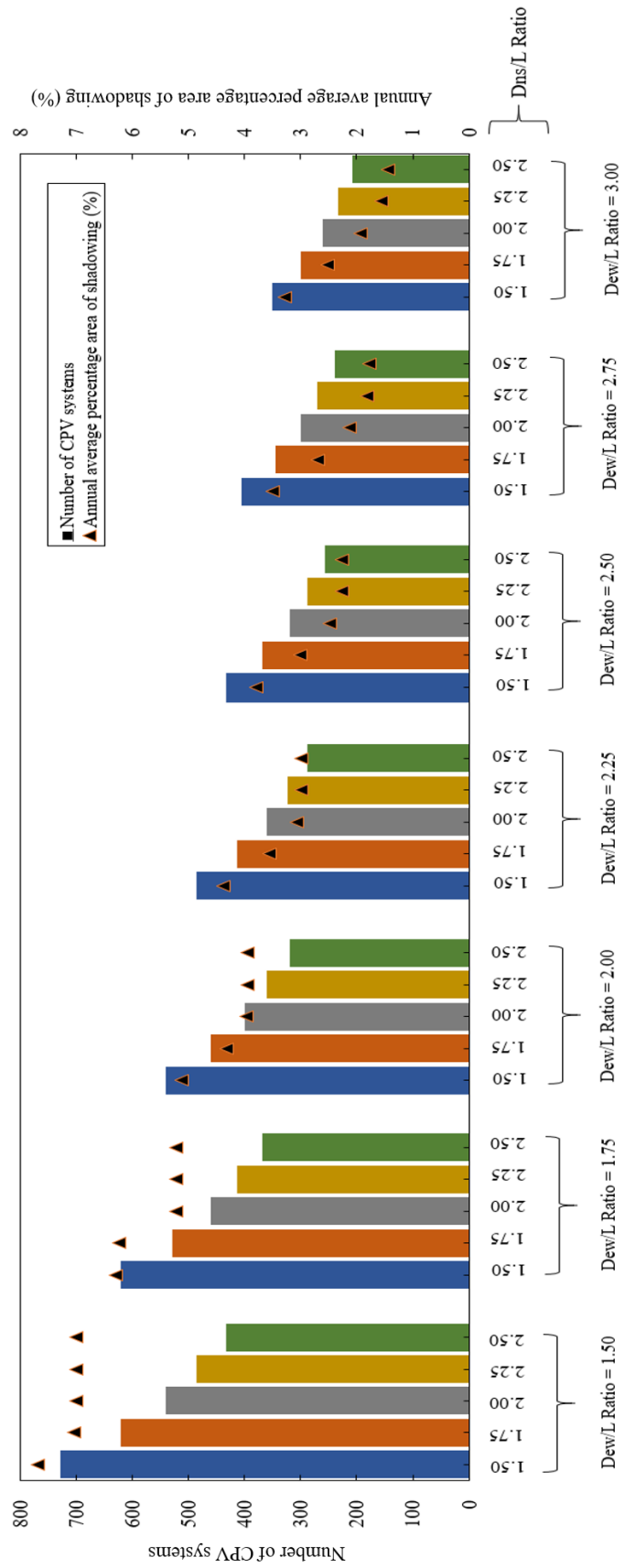


Figure 4.1: The annual average percentage of shadowing area (%) for square array layout.

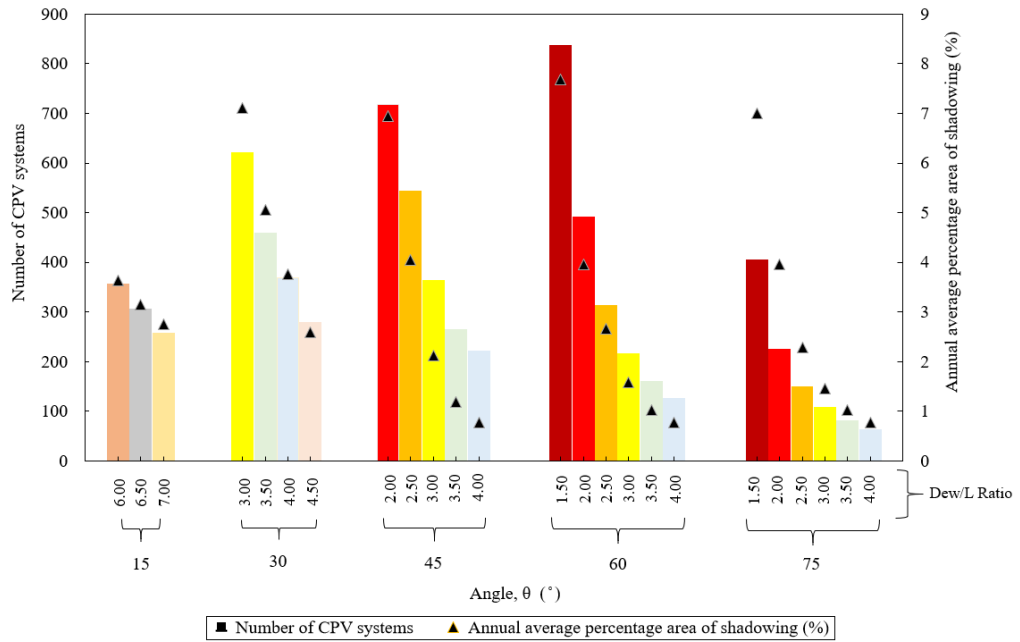


Figure 4.2: The annual average percentage of shadowing area (%) for staggered array layout. The results were taken from its minimum D_{ew}/L ratio for each angle to avoid collision between adjacent CPV systems. The iteration of simulation algorithm will not be continued when the LCOE increases with the increment in the D_{ew}/L ratio to save the computational time.

4.2 Annual energy generation

The annual energy generated by the solar farm consisted of CPV systems is also simulated by taking the shadowing effect into consideration for every 15 minutes throughout the year, where the average global horizontal irradiation of Kota Kinabalu is 1800 kWh/m². The simulated results of annual energy generation for both the square array and staggered array layout configurations are depict in Figures 4.3 and 4.4 respectively with the assumption that LAR is 1 and the land cost is US\$ 12.81 per square meter within the specified land area of 62,500 m².

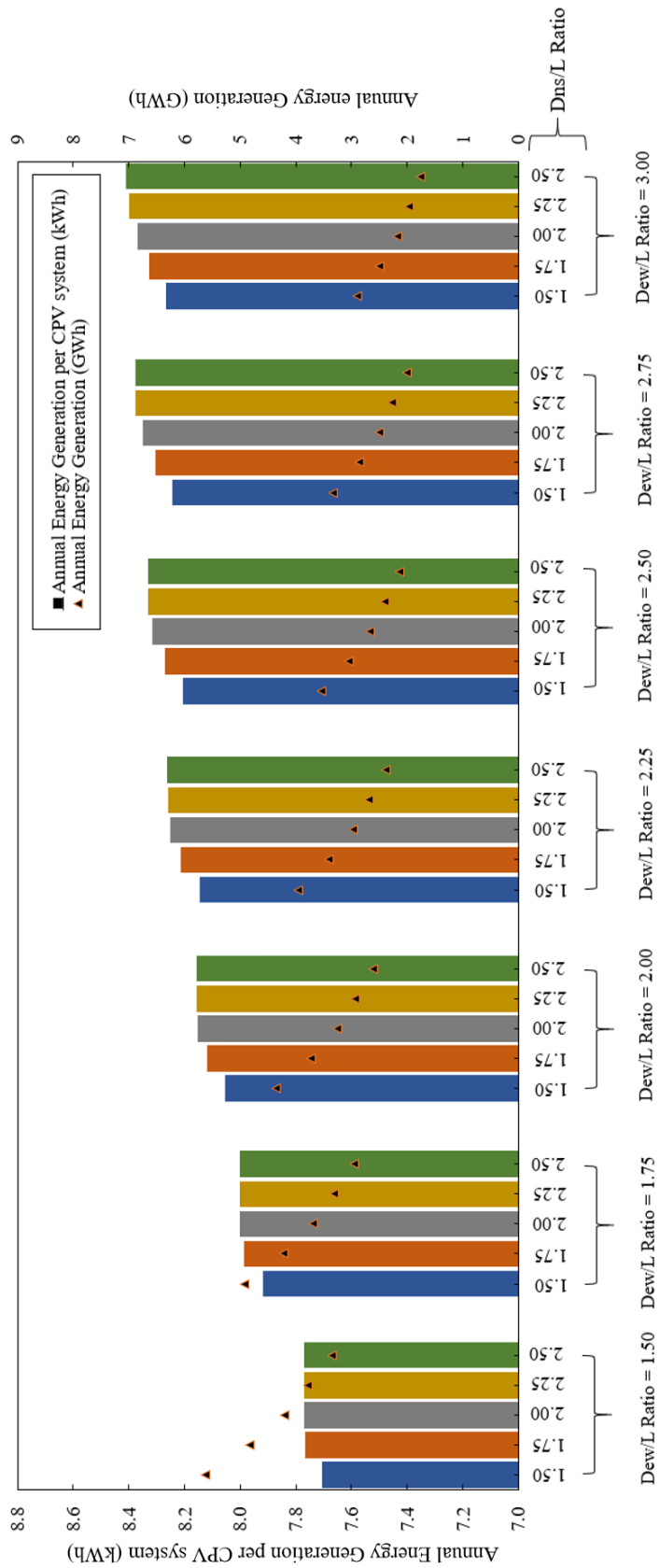


Figure 4.3: The annual energy generation per CPV system (kWh) and the annual energy generation (GWh) for square array layout.

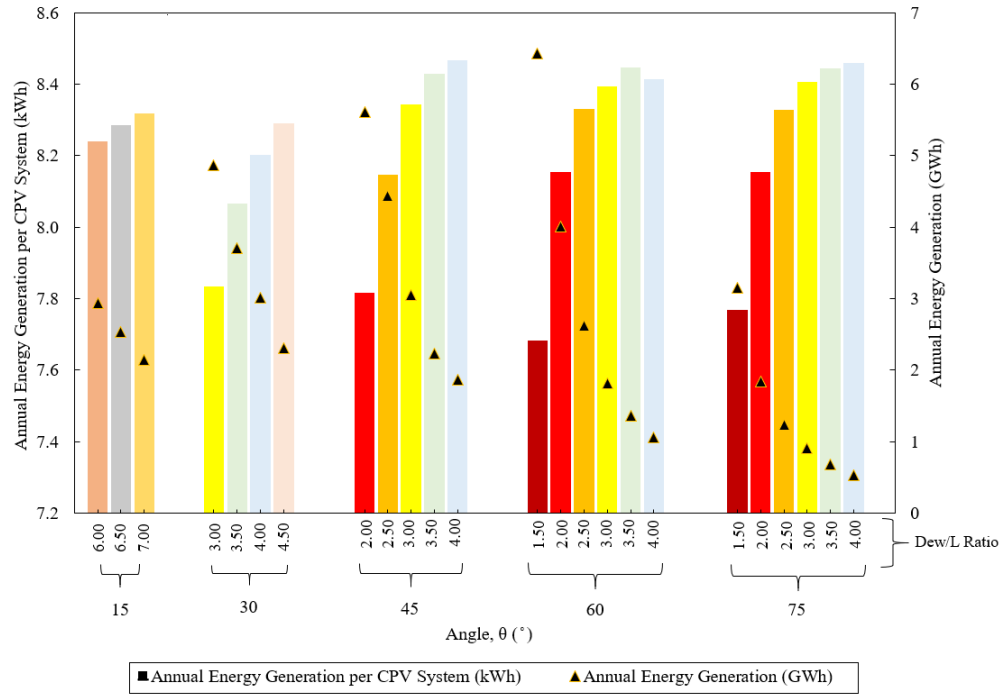


Figure 4.4: The annual energy generation per CPV system (kWh) and the annual energy generation (GWh) for staggered array layout. The results were taken from its minimum D_{ew}/L ratio for each angle to avoid collision between adjacent CPV systems. The iteration of simulation algorithm will not be continued when the LCOE increases with the increment in the D_{ew}/L ratio to save the computational time.

The annual energy generation for each CPV system is directly proportional to D_{ew}/L and D_{ns}/L ratios for the square array layout configuration due to the increase in spacing between any two adjacent CPV systems. This reduces the shadowing effect, and therefore increase the energy generation for each CPV system. On the other hand, the annual energy generation of the CPV field is inversely proportional to both D_{ew}/L and D_{ns}/L ratios since the total

quantity of CPV systems that can be allocated in the designated area is reduced. As for the staggered array layout configuration, similar pattern is seen from the graph as that of the square array layout, i.e.: (1) the annual energy generation for each CPV system is directly proportional to D_{ew}/L ratios; (2) the annual energy generation by the CPV field is inversely proportional to D_{ew}/L .

According to Figures 4.3 and 4.4, the shorter distance between CPV systems can increase the annual energy generation of the CPV field within the specified area. However, this approach will need to increase the number of CPV systems to be allocated in the solar farm which will also indirectly increases the investment cost of the solar farm. Moreover, this approach will also cause a significant reduction in the energy conversion efficiency for each CPV system since it has high packing factor with higher impact of shadowing effect. The LCOE of the CPV system solar farm must be reduced in order to compete with the LCOE of the conventional power generation plants. This is needed to garner more interest of investment in solar power installations. Thus, it is important to determine the energy production per unit cost in term of the LCOE to evaluate the optimal layout design and also the economic feasibility of solar farm.

4.3 Levelized cost of electricity (LCOE)

The LCOE is taken into consideration in the layout design of CPV field in order to identify the most optimized value for: (1) both the D_{ew}/L and D_{ns}/L ratios in the case study of square array layout configuration, or; (2) the most optimized values for D_{ew}/L ratio and spacing ratio in the case study of staggered array layout configuration. Based on the specification listed in Table 4.3, the LCOE

are simulated for the square array and the staggered array layout configurations. The simulated results of LCOE for both square array and staggered array layout configurations are depicted in Figures 4.5 and 4.6 respectively. In this research paper, the interest expenditure is assumed to be zero since no loan is applied to finance this solar power plant and there is no incentive considered.

According to the results shown in both Figures 4.5 and 4.6, the results show that the optimal square array layout in this case study is at D_{ew}/L ratio of 2.75 and D_{ns}/L ratio of 1.50, which give the lowest LCOE value of US\$ 0.2289/kWh, whereas the optimal staggered array layout design is determined at D_{ew}/L ratio of 2.50 and spacing angle of 45 degree, which has a LCOE value of US\$ 0.2197/kWh. It is fascinating to see that the respective annual average percentage area of shadowing is not the lowest in the aforementioned cases. For the case of staggered array layout, the iteration of simulation algorithm will not be continued when the LCOE increases with the increment in the D_{ew}/L ratio in order to save the computational time.

Table 4.3: The parameters required in the calculation of LCOE of the solar farm consisted of CPV systems.

Land leasing @ US\$ 12.81/m ²	US\$ 800,625
Excavation and preparation of land	US\$ 23809.52
Discount rate	3%
Degradation rate	0.5%
Lifespan of CPV system, t	25 years
Interest expenditure for t years	0%
Construction and installation cost per CPV tracker (Fraunhofer ISE, 2015)	US\$ 26249.14
Operations and maintenance cost of solar system (Wright, Badruddin and Robertson-Gillis, 2018)	US\$ 14/kW-yr

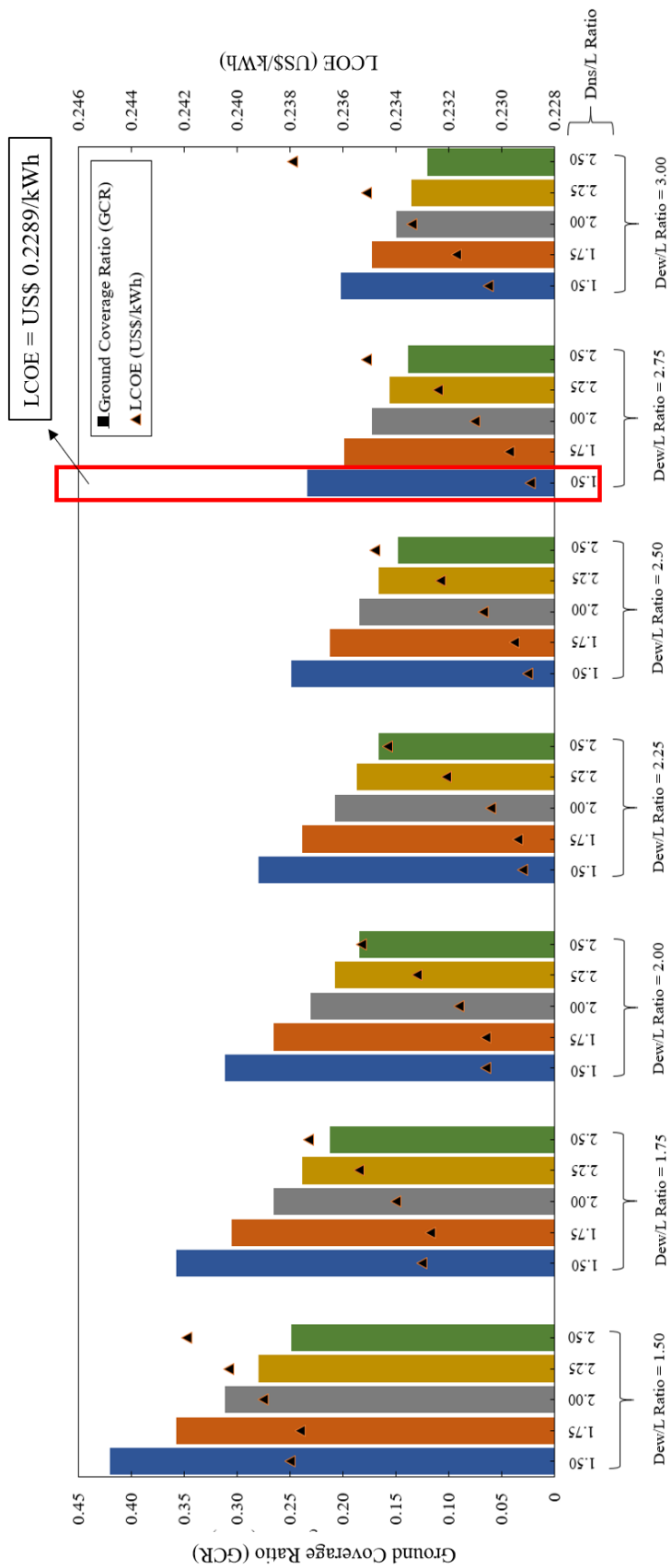


Figure 4.5: The ground coverage ratio (GCR) and LCOE (US\$/kWh) for square array layout at LAR = 1.

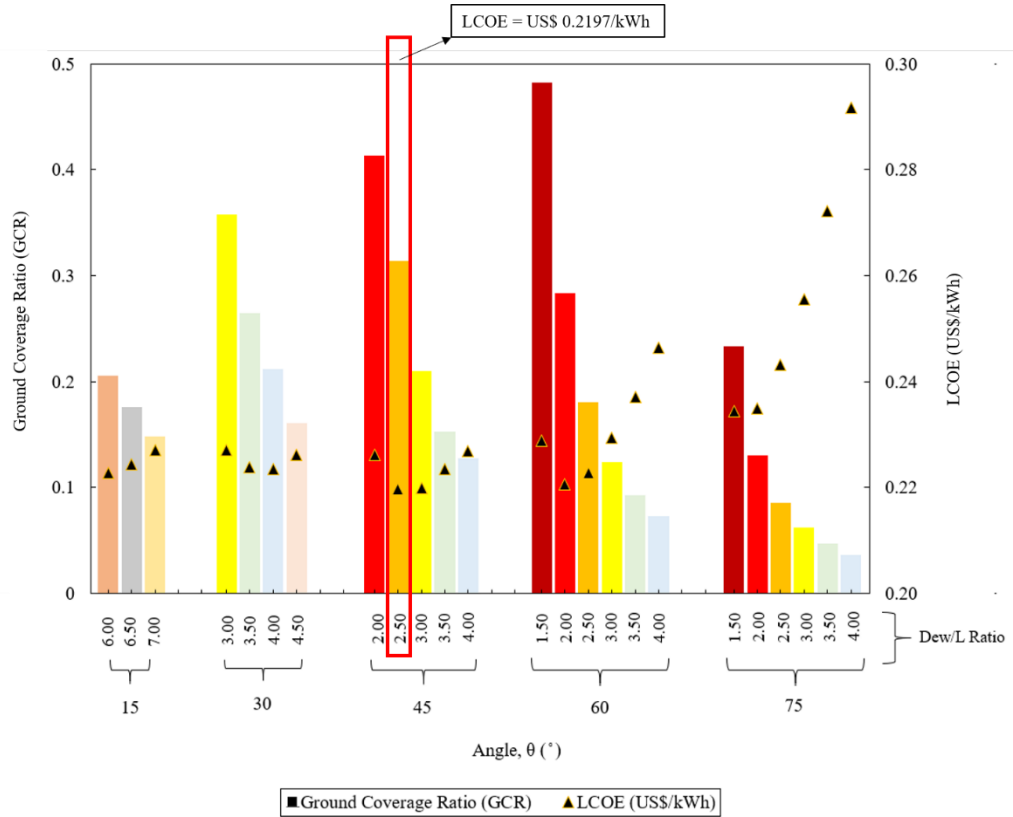


Figure 4.6: The ground coverage ratio (GCR) and LCOE (US\$/kWh) for staggered array layout at LAR = 1. The results were taken from its minimum D_{ew}/L ratio for each angle to avoid collision between adjacent CPV systems. The iteration of simulation algorithm will not be continued when the LCOE increases with the increment in the D_{ew}/L ratio to save the computational time.

According to the simulation results, it is crucial to take LCOE into consideration during the optimization of the field layout design in order to determine the minimum cost of electricity per kWh for the solar power plant project. According to both the simulation results of square array layout and staggered array layout configurations, the staggered array layout configuration is found to be the most optimal layout design for the solar power plant since it has a lower LCOE value than that of square array layout configuration. Thus,

the optimized layout design is the staggered array layout configurations with the lowest value of LCOE at D_{ew}/L ratio of 2.50 and spacing angle of 45 degree at which the LAR = 1 and the specified land area is 62,500 m². It will be difficult to make comparison between our algorithm and methods used by other researchers as the research are of different approach. In this case, we use the LCOE instead of the shadowing effect to perform field layout design optimization. The methodology introduced in this research can referred by investors and engineers as a tools or guideline to perform optimization of field layout design of the solar power plant with the lowest value of LCOE.

4.4 Edge effect

There are many previous case studies have been done by other researchers without the consideration of the edge effect for the modelling of solar power plant. Their research assumed that all CPV systems are surrounded by the same amount of adjacent CPV systems. This also applies to those CPV systems which are placed at the edge of the solar farm. Thus, additional studies are carried out in this research to find out if it is necessary to consider edge effect into the field layout optimization. The simulation results obtained for the annual energy generation and LCOE as shown in Figures 4.3, 4.4, 4.5 and 4.6 are obtained by considering edge effect. In order to perform a comparison study, the simulation for the annual energy generation and LCOE is done without taking the edge effect into consideration. The optimum layout configuration of square array and staggered array layout configuration are shown in Table 4.4 with and without the consideration of edge effect.

It was found that the square array layouts with and without the consideration of edge effect came to the same optimum layout configurations. However, there are differences in their annual energy generation and the value of LCOE. There is a percentage difference of 0.30% for the value of LCOE between the cases with and without edge effect whereas the percentage difference in the annual energy generation is 30% for the square array layout. The annual energy generation with the consideration of edge effect is 3.3381 GWh which is slightly higher than the annual generation without the consideration of edge effect of 3.3279 GWh. Contrarily, the LCOE without considering the edge effect is US\$ 0.2296/kWh at which is slightly higher than the LCOE of US\$ 0.2289/kWh with the consideration of edge effect. This is due to the overestimation of shadowing effect in the modelling of solar farm for the case of without edge effect consideration, especially those CPV systems placed near to the edge of the solar farm causing lower annual energy generation. The percentage differences between the annual energy generation of the CPV field with and without the consideration of the edge effect with the same layout configuration parameters setting (D_{ew}/L and D_{ns}/L) are ranges between 0.11% and 0.44% for the square array layout configuration.

According to the results tabulated in Table 4.4, a different optimized staggered array layout configuration is observed for the cases with and without consideration of edge effect. The optimized staggered array layout configuration without the consideration of edge effect is observe to have the layout configuration of $D_{ew}/L = 3.00$ and spacing angle = 45° whereas the optimized staggered array layout configuration with the consideration of edge effect is observe at the layout configuration of $D_{ew}/L = 2.50$ and spacing angle = 45° . The

case of the edge effect consideration has shown a significant higher amount of annual energy generation that is 4.4400 GWh as compared to 3.0397 GWh in the case of without the edge effect consideration for the optimized staggered array layout. Contrarily, the value of LCOE without the consideration of the edge effect is US\$ 0.2202/kWh which is slightly higher than US\$ 0.2197/kWh of the case with consideration of the edge effect. The comparison between the cases of staggered array optimized layout configuration with and without the consideration of the edge effect has displayed a small difference of 0.23% in LCOE but there is an obvious difference of 31.53% in annual energy generation. The optimum east-west distance between adjacent panels is closer to each other is observed when considering the edge effect, and this led to a significant increase of 31.53% in annual energy generation as compared to the optimum layout configuration without considering the edge effect. The percentage differences between annual energy generation of the CPV staggered array layout configuration for with and without the consideration of the edge effect with the same layout configuration parameters setting (D_{ew}/L and θ) which ranges between 0.05% and 0.56%. Based on several observation in the results of this research study, it is recommended to consider the edge effect into the simulation of annual energy generation and LCOE as there is a significant impact of this edge effect to the modelling of solar power plant. Thus, it is proven that the edge effect is crucial to be considered in the layout configuration optimization process.

Table 4.4: The optimal layout configuration for the cases of with and without considering the edge effect in the solar farm modelling.

	Layout Configuration	Parameters		Annual Energy Generation (GWh)	LCOE (US\$/kWh)
Square Array Layout	Without edge effect	D_{ew}/L	D_{ns}/L	3.3279	0.2296
		2.75	1.50		
	With edge effect	D_{ew}/L	D_{ns}/L	3.3381	0.2289
		2.75	1.50		
Staggered Array Layout	Without edge effect	D_{ew}/L	Angle, θ	3.0397	0.2202
		3.00	45		
	With edge effect	D_{ew}/L	Angle, θ	4.4400	0.2197
		2.50	45		

4.5 Land-related cost

According to section 4.3, the optimal layout configuration of a solar power plant can be determined as long as the computed LCOE is of the lowest value. Another additional study has been carried out by varying the land leasing cost with the exact same specified land area of 62,500 m² for both the square array and staggered array layout configurations in order to explore and discover how do the land-related cost influences the optimal layout configuration and the LCOE value of a solar power plant. Therefore, a list of simulations is conducted for several land leasing cost, i.e. RM 5 per sq. ft. (US\$ 12.81 per sq. meter), RM 10 per sq. ft. (US\$ 25.63 per sq. meter), RM 15 per sq. ft. (US\$ 38.44 per sq. meter), RM 20 per sq. ft. (US\$ 51.26 per sq. meter), RM 25 per sq. ft. (US\$ 64.07 per sq. meter), and RM 30 per sq. ft. (US\$ 76.89 per sq. meter).

The results obtained from the simulation are tabulated in Table 4.5. Overall, the LCOE for both the optimal square array and staggered array layout

configurations increases as the cost of land lease increases. In addition, the optimum square array and staggered array layout configurations vary at different land leasing cost. The spacing distance between any two CPV systems for the optimum square array and staggered array layout configuration reduces when the cost of land lease increases. However, this land leasing cost may be unavoidably expensive since the land is scarce in some of the countries. Therefore, the results of the simulation have shown that it will be great to reduce the spacing distance between CPV systems for a lower LCOE value although the energy generation for each CPV system will be lower due to higher amount of shadowing effect. Besides, the optimal ground coverage ratio (GCR) also increases as the cost of land lease become higher. There are more CPV systems installed in the specified land area for the case with higher GCR. Thus, the annual energy generation also increase proportionally. These results have proven that the LCOE and the optimal layout configuration of the whole solar power plant will be affected by different land leasing cost.

4.6 Land aspect ratio (LAR)

In all the aforementioned case studies in this research, the land aspect ratio (LAR) is specifically set to one ($LAR = 1$) at which the size of land modelled a perfect square. However, it will be very much dependent on the availability and landscape of the land in practical. The LAR of the solar farm is actually quite complicated to be analyzed in a comprehensive scientific approach as each and every setting of LAR involves labour intensive and complicated design of CPV field which also need to provide the optimization of various parameters at the

same time. In spite of that, it is emphasized in this research study that the LAR actually influenced the CPV field performance. There will be three case studies mentioned in this section, i.e. LAR of 0.5, 1.0 and 2.0 has been selected to observe its impact towards the annual energy generation and LCOE at the total land area of 62,500 m² with the land cost of US\$ 12.81/m². The optimal square array and staggered array layout configurations have simulated to achieve the lowest LCOE in each respective layout of solar farm as depicted in Figure 4.7.

According to the results simulated and depicted in Figure 4.7, the optimum square array layout configuration which provides the lowest LCOE for LAR of 0.5, 1 and 2 are $D_{ew}/L = 2.25$ and $D_{ns}/L = 1.50$, $D_{ew}/L = 2.75$ and $D_{ns}/L = 1.50$, and $D_{ew}/L = 2.50$ and $D_{ns}/L = 1.50$ respectively. Whereas, the optimum staggered array layout configuration which give lowest LCOE for LAR of 0.5, 1 and 2 are $D_{ew}/L = 3.50$ with spacing angle = 30°, $D_{ew}/L = 2.50$ with spacing angle = 45° and $D_{ew}/L = 3.00$ with spacing angle = 45° respectively. This shows that the optimum square array and staggered array layout configurations are greatly dependent on the LAR. In addition, the results simulated have also displayed that the staggered array layout configuration has lower value of LCOE than that of the square array layout configuration for all the three case which considers LAR. As a result, the LAR is also one of the essential variables which can influence the optimal layout configuration of a solar power plant. Based on Figure 4.7, we can see that our most optimum configuration is staggered array with the GCR of 0.46 which is much higher than when we are to compare it with the best configuration in the other research work conducted by Díaz-Dorado, Cidrás and Carrillo (Díaz-Dorado, Cidrás and Carrillo, 2017) at which their optimum configuration's GCR is 0.33. This once again proves that it is important

to use LCOE as a factor to optimize the layout configuration of a solar power plant instead of the shadowing effect.

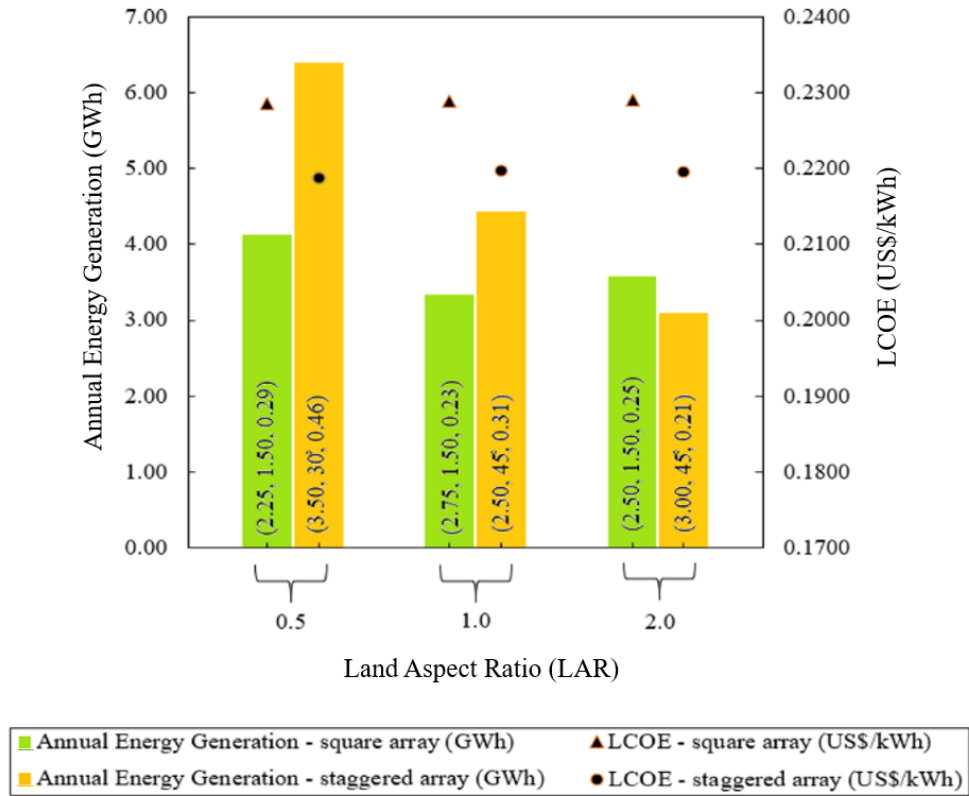


Figure 4.7: The relationship between the annual energy generation, LCOE, square array layout configuration (D_{ew}/L , D_{ns}/L , GCR) and staggered array layout configuration (D_{ew}/L , Angle, GCR) at different LAR.

CHAPTER 5

CONCLUSION AND FUTURE WORK

5.1 Conclusion

The optimization of the layout design of solar power plant (SPP) which utilized a systematic approach using computational algorithm has been proposed with the consideration of local weather data, land aspect ratio, shadowing efficiency, energy generation, LCOE and land cost. The methodology also has been developed in this research study as to analyze the shadowing effect of CPV system which utilized two-axis tracking system. The simulation results in this research shows that the CPV systems arranged in staggered array layout of the solar power plant has the lowest value of LCOE at a D_{ew}/L ratio of 2.50 and spacing angle of 45 degree despite the fact that its annual average percentage area of shadowing is not the lowest. Besides, the simulation in this research work also proved that there are several other factors, i.e. the land-related cost, edge effect and LAR, can also influence the selection of optimal layout configuration and also the LCOE of the SPP. Therefore, it is significant to include the edge effect and LCOE as the key factors in the layout design in order to attain the comprehensive economic balance between cost and power generation. In conclusion, the aforementioned methodology can be applied to aid researchers and engineers in the optimization of the solar field layout design of the CPV systems, to reach the lowest investment in term of LCOE.

5.2 Future work

Since this research work was to produce a methodology to assist researchers and engineers to optimize the field layout design of the CPV systems, to achieve the lowest investment in term of LCOE. It would be great to do a Graphic User Interface (GUI) using MATLAB simulation platform or other relevant platform as this can help to implement the aforementioned methodology into a simple visual feedback for a more user-friendly purpose. Moreover, this can also provide higher productivity and better accessibility to captivate more potential researchers or engineers to use this in their researches or projects.

REFERENCES

- Abdallah, S. (2004) 'The effect of using sun tracking systems on the voltage–current characteristics and power generation of flat plate photovoltaics', *Energy Conversion and Management*. Pergamon, 45(11–12), pp. 1671–1679. doi: 10.1016/J.ENCONMAN.2003.10.006.
- Amarjeet, S. J. (2013) *Solar tracking system - Report*. Available at: <https://www.slideshare.net/ASJamwal/solar-tracking-system-report> (Accessed: 8 June 2020).
- Belhachat, F. and Larbes, C. (2015) 'Modeling, analysis and comparison of solar photovoltaic array configurations under partial shading conditions', *Solar Energy*. Pergamon, 120, pp. 399–418. doi: 10.1016/J.SOLENER.2015.07.039.
- Branker, K., Pathak, M. J. M. and Pearce, J. M. (2011) 'A review of solar photovoltaic levelized cost of electricity', *Renewable and Sustainable Energy Reviews*, 15(9), pp. 4470–4482. doi: 10.1016/j.rser.2011.07.104.
- Chong, K.-K. and Wong, C.-W. (2010) 'General Formula for On-Axis Sun-Tracking System', in *Solar Collectors and Panels, Theory and Applications*. Sciyo. doi: 10.5772/10341.
- Chong, K. K. and Tan, M. H. (2012) 'Comparison study of two different sun-tracking methods in optical efficiency of heliostat field', *International Journal of Photoenergy*, 2012. doi: 10.1155/2012/908364.
- Chong, K. K. and Wong, C. W. (2008) 'General formula for on-axis sun-tracking system and its application in improving tracking accuracy of solar collector', *Solar Energy*, 83, pp. 298–305. doi: 10.1016/j.solener.2008.08.003.

Cumpston, J. and Pye, J. (2014) 'Shading and land use in regularly-spaced sun-tracking collectors', *Solar Energy*, 108, pp. 199–209. doi: 10.1016/j.solener.2014.06.012.

D. Nagesh, M. Ramesh (2015) *Solar Photovoltaic Panels Tracking System, IJSRD-International Journal for Scientific Research & Development*/. Available at: www.ijrsrd.com (Accessed: 8 June 2020).

Dähler, F., Ambrosetti, G. and Steinfeld, A. (2017) 'Optimal solar dish field layouts for maximum collection and shading efficiencies', 144, pp. 286–294. doi: 10.1016/j.solener.2017.01.024.

Dawson, S. (2013) *Sustainable by design, Drapers*. doi: 10.1111/j.1948-7169.1998.tb00218.x.

Díaz-Dorado, E., Cidrás, J. and Carrillo, C. (2017) 'A method to estimate the energy production of photovoltaic trackers under shading conditions', *Energy Conversion and Management*. Elsevier, 150(August), pp. 433–450. doi: 10.1016/j.enconman.2017.08.022.

Edgar, R., Stachurski, Z. and Cochard, S. (2016) 'Optimising direct normal insolation of rectangular PV platforms', *Solar Energy*. Elsevier Ltd, 136, pp. 166–173. doi: 10.1016/j.solener.2016.06.072.

Edwards, B. P. (1978) 'Shading and spacing in paraboloidal collector arrays', *Solar Energy*. Pergamon, 21(5), pp. 435–439. doi: 10.1016/0038-092X(78)90177-9.

Eke, R. and Senturk, A. (2012) 'Performance comparison of a double-axis sun tracking versus fixed PV system', *Solar Energy*, 86(9), pp. 2665–2672. doi:

10.1016/j.solener.2012.06.006.

Fraunhofer ISE (2015) ‘Current and Future Cost of Photovoltaics: Long-term Scenarios for Market Development.’, p. 82.

Gómez-Gil, F. J., Wang, X. and Barnett, A. (2012) ‘Energy production of photovoltaic systems: Fixed, tracking, and concentrating’, *Renewable and Sustainable Energy Reviews*. Elsevier Ltd, pp. 306–313. doi:

10.1016/j.rser.2011.07.156.

Gordon, J. M. and Wenger, H. J. (1991) ‘Central-station solar photovoltaic systems: Field layout, tracker, and array geometry sensitivity studies’, *Solar Energy*. Pergamon, 46(4), pp. 211–217. doi: 10.1016/0038-092X(91)90065-5.

Green, M. A. *et al.* (2016) ‘Solar cell efficiency tables (version 47)’, *Progress in Photovoltaics: Research and Applications*. John Wiley and Sons Ltd, pp. 3–11. doi: 10.1002/pip.2728.

Green, M. A. *et al.* (2019) ‘Solar cell efficiency tables (version 54)’, (May), pp. 565–575. doi: 10.1002/pip.3171.

Honsberg, C. (2015) *Solar Time | PVEducation*. Available at:

<https://www.pveducation.org/pvcdrom/properties-of-sunlight/solar-time>

(Accessed: 8 June 2020).

Hu, Y. and Yao, Y. (2016) ‘A methodology for calculating photovoltaic field output and effect of solar tracking strategy’, *Energy Conversion and Management*. Pergamon, 126, pp. 278–289. doi:

10.1016/J.ENCONMAN.2016.08.007.

Johnson-Hoyte, D. *et al.* (no date) *Dual-Axis Solar Tracker: Functional Model Realization and Full-Scale Simulations Picture of the Functional Model Picture of a Simulation Picture of a Simulation.*

Lorenzo, E., Narvarte, L. and Muñoz, J. (2011) 'Tracking and back-tracking', *Progress in Photovoltaics: Research and Applications*. John Wiley & Sons, Ltd, 19(6), pp. 747–753. doi: 10.1002/pip.1085.

Lovegrove, K. *et al.* (2013) 'Photovoltaics under concentrated sunlight Concentrating solar cells', *Solar Energy*. Elsevier Ltd (Woodhead Publishing Series in Energy), 2(3–4), pp. 2803–2827. doi: 10.1002/pip.

Meller, Y. and Kribus, A. (2013) 'Kaleidoscope homogenizers sensitivity to shading', *Solar Energy*. Pergamon, 88, pp. 204–214. doi: 10.1016/J.SOLENER.2012.11.010.

Mousazadeh, H. *et al.* (no date) 'A review of principle and sun-tracking methods for maximizing solar systems output'. doi: 10.1016/j.rser.2009.01.022.

Muñoz, E. *et al.* (2010) 'CPV standardization: An overview', *Renewable and Sustainable Energy Reviews*, 14(1), pp. 518–523. doi: 10.1016/j.rser.2009.07.030.

Narvarte, L. and Lorenzo, E. (2008) 'Tracking and ground cover ratio', *Progress in Photovoltaics: Research and Applications*. John Wiley & Sons, Ltd, 16(8), pp. 703–714. doi: 10.1002/pip.847.

National Renewable Energy Laboratory (no date) *Solar Energy Basics / NREL*. Available at: <https://www.nrel.gov/workingwithus/re-solar.html> (Accessed: 8

June 2020).

Oliveira Fartaria, T. and Collares Pereira, M. (2013) ‘Simulation and computation of shadow losses of direct normal, diffuse solar radiation and albedo in a photovoltaic field with multiple 2-axis trackers using ray tracing methods’, *Solar Energy*, 91, pp. 93–101. doi: 10.1016/j.solener.2013.02.008.

Pérez-Higueras, P. *et al.* (2015) ‘Thin photovoltaic modules at ultra high concentration’, *AIP -11th International Conference on Concentrator Photovoltaic Systems*, 130004(1679), p. 130004. doi: 10.1063/1.4931564.

Perpiñán, O. (2012) ‘Cost of energy and mutual shadows in a two-axis tracking PV system’, *Renewable Energy*, 43, pp. 331–342. doi: 10.1016/j.renene.2011.12.001.

Pons, R. L. and Dugan, A. F. (1984) ‘The Effect of Concentrator Field Layout on the Performance of Point-Focus Distributed Receiver Systems’, *Journal of Solar Energy Engineering*, 106(1), p. 35. doi: 10.1115/1.3267559.

PVPerformance Modeling collaborative (no date) *PV Performance Modeling Collaborative / Sun Position*. Available at: <https://pvpmc.sandia.gov/modeling-steps/1-weather-design-inputs/sun-position/solar-position-algorithm-spa/%0Ahttps://pvpmc.sandia.gov/modeling-steps/1-weather-design-inputs/sun-position/> (Accessed: 8 June 2020).

Rockwell Automation (2011) *Solar Tracking Application Example: Single Axis Tracker used for Solar Photovoltaic (PV) Panel Applications Example: Single Axis Tracker used for Solar Thermal Parabolic Trough Applications*. Available at:

https://literature.rockwellautomation.com/idc/groups/literature/documents/wp/0em-wp009_-en-p.pdf (Accessed: 8 June 2020).

solarflexrack (2013) *Single-Axis and Dual-Axis Tracking: Advantages and Disadvantages – Solar FlexRack*. Available at: <http://solarflexrack.com/single-axis-and-dual-axis-tracking-advantages-and-disadvantages/> (Accessed: 8 June 2020).

Swetansh (2013) *Dual Axis Solar Tracker Using Ldr As a Sensor*. Available at: <https://www.slideshare.net/sweetwetansh/solar-tracker-report-swetansh> (Accessed: 8 June 2020).

Tan, M. H. and Chong, K. K. (2016) ‘Influence of self-weight on electrical power conversion of dense-array concentrator photovoltaic system’, *Renewable Energy*. Elsevier Ltd, 87, pp. 445–457. doi: 10.1016/j.renene.2015.10.022.

U.S. Department of Energy (2014) *Learn more at energy.gov/betterbuildings On-Site Commercial Solar PV Decision Guide*.

Wright, D. J., Badruddin, S. and Robertson-Gillis, C. (2018) ‘Micro-Tracked CPV Can Be Cost Competitive With PV in Behind-The-Meter Applications With Demand Charges’, *Frontiers in Energy Research*, 6(September), pp. 1–15. doi: 10.3389/fenrg.2018.00097.

Zip, K. (2013) *What is a solar tracker?*, *Solar Power World*. Available at: <https://www.solarpowerworldonline.com/2013/04/how-does-a-solar-tracker-work/> (Accessed: 8 June 2020).

PUBLICATIONS

According to the findings from this research work, two paper has been published. The detail on the full published conference paper through International Conference on Sustainable Energy and Green Technology 2018 [1] and the published journal paper through Solar Energy Journal [2] was shown below:

[1] Oon, L.V., Tan, M.H., Wong, C.W., Yew, T.K., Chong, K.K., Tan, W.C., Lim, B.H., 2019. Space optimization of concentrator photovoltaic systems based on levelized cost of electricity in solar power plant.

[2] Oon, L.V., Tan, M.H., Wong, C.W., Chong, K.K., 2020. Optimization study of solar farm layout for concentrator photovoltaic system on azimuth-elevation sun-tracker.

*Note: The data and figures in both the papers mentioned above were repeated in this dissertation since the publications are of the same research study as described in this dissertation. Both publications are written by the author of this dissertation.